

## Janus particles: design, preparation, and biomedical applications

H. Su <sup>a,d</sup>, C.-A. Hurd Price <sup>b,c,d</sup>, L. Jing <sup>b</sup>, Q. Tian <sup>b</sup>, J. Liu <sup>b,c,\*\*</sup>, K. Qian <sup>a,\*</sup>



<sup>a</sup> School of Biomedical Engineering, Med-X Research Institute, Shanghai Jiao Tong University, Shanghai 200030, China

<sup>b</sup> State Key Laboratory of Catalysis, Dalian Institute of Chemical Physics, Chinese Academy of Sciences, Dalian 116023, China

<sup>c</sup> DICP-Surrey Joint Centre for Future Materials, Department of Chemical and Process Engineering, University of Surrey Guildford, Surrey, GU2 7XH, United Kingdom

### ARTICLE INFO

**Keywords:**  
Biomedical engineering  
Drug delivery  
Bio-imaging  
Bio-sensing

### ABSTRACT

Janus particles with an anisotropic structure have emerged as a focus of intensive research due to their diverse composition and surface chemistry, which show excellent performance in various fields, especially in biomedical applications. In this review, we briefly introduce the structures, composition, and properties of Janus particles, followed by a summary of their biomedical applications. Then we review several design strategies including morphology, particle size, composition, and surface modification, that will affect the performance of Janus particles. Subsequently, we explore the synthetic methodologies of Janus particles, with an emphasis on the most prevalent synthetic method (surface nucleation and seeded growth). Following this, we highlight Janus particles in biomedical applications, especially in drug delivery, bio-imaging, and bio-sensing. Finally, we will consider the current challenges the materials face with perspectives in the future directions.

### 1. Introduction

Janus particles, named after a two-faced Roman God of the same name, were suggested by Pierre-Gilles de Gennes when he made his Nobel Laureate speech to the scientific community in 1991 [1]. Since then, various Janus particles (JPs) have been synthesized, and the definition of JPs is extended far beyond the initial two-faced amphiphilic structure [2,3]. JPs have become objects composed of two or more parts that differ in their physical and chemical properties, often contrary in nature [2–6]. The anisotropic structure of JPs contains optical, electrical, or magnetic properties etc., which facilitate JPs with many advantages, such as multifunctional properties and ease of modification [3,6–10]. Although individual components combine and coexist together in a single-particle system, the intrinsic chemical, magnetic, optical, and electronic properties of each domain are seldom altered or lost [11–15], allowing the unique properties of different parts to contribute in improving the chemical and physical properties of the whole. Following surface modification, functionally distinct surfaces of the JPs can be used to selectively conjugate specific chemical moieties [2,16–18]. Therefore, JPs have attracted tremendous attention in recent years and exhibited great potential in numerous applications including interfacial stabilizers, catalysis, electrochemical applications, biomedicine etc. [3,12,19–22].

In the past two decades, JPs with various morphologies have been designed and prepared, ranging from simple spherical particles to different shapes, such as dumbbell-shape [23,24], snowman-shape [25–27], disk-shape [28,29], rod-shape [30–32], half-raspberry-shape [21,33,34], and mushroom-shape [35,36]. The general division of JPs may be considered as polymeric, inorganic, and polymeric-inorganic compositions [2,3,12]. It is well known that properties and applications of JPs rely strongly on their morphology with defined size and chemical composition, in addition to surface chemistry, which are important factors that affect the performance of JPs [2,3,37,38]. Various synthetic strategies have been explored for the fabrication of JPs demonstrating high degrees of control over physical characteristics, material composition, and surface chemistry. These methods include phase separation, masking, self-assembly, surface nucleation and seeded growth, and microfluidics etc. [3,6,39]. The surface nucleation and seeded growth method is the most suitable for the synthesis of complex morphologies, so much so that it has become the most prevalent method for the construction of JPs.

JPs with well-controlled anisotropic structure have attracted increased interest in various fields, particularly in biomedical applications [8,22,40,41]. Although many isotropic particles present excellent performance in biomedical field [42–46], JPs play irreplaceable roles due

\* Corresponding author.

\*\* Corresponding author.

E-mail addresses: [jian.liu@surrey.ac.uk](mailto:jian.liu@surrey.ac.uk) (J. Liu), [k.qian@sjtu.edu.cn](mailto:k.qian@sjtu.edu.cn) (K. Qian).

<sup>d</sup> These authors contributed equally to this work.

to their asymmetric compositions and independent functions. One promising biomedical application is drug delivery, where a single JP material with multiple domains can simultaneously realize multidrug loading and serve as an ideal carrier [40,47,48]. The JPs can be tailored to the desired drugs, to ensure any opposing properties (e.g. hydrophilicity/hydrophobicity, acidity/basicity, etc.) can remain separated. Moreover, the separate compartments of the JPs can be modified with diverse functional molecules for separate control over the drug release [47]. If the components are magnetic, optical or metallic, the JPs can be used for magnetic resonance imaging (MRI), optical imaging (OI) or computed tomography (CT) and achieve single/multiple imaging-guided therapy [5,49,50]. Furthermore, JPs have been developed for bio-sensing. Biomolecules (enzyme, antibody, etc.) or chemical groups are modified on one side of JPs for the recognition of analytes (protein, cells, bacteria, etc.), and the other side is composed of an optical or magnetic material. For these functional JPs that can serve as biosensors for the detection of biomolecules, cells or bacteria [16,51,52]. Nano- or micro motors constructed by JPs are also promising candidates for biomedical applications. These Janus motors can be driven by light, bubble or a magnetic field while simultaneously completing capture/adsorption of targets due to its unique composition and structure [22, 40,53]. A few Janus motors are even capable of self-destruction following the completion of their function, disassembling into biocompatible and harmless components [54].

Herein, we introduce a few design strategies of JPs capable of well-controlled morphology, particle size, composition, and surface modification. Subsequently, we review the common synthetic methods of JPs, mainly focusing on the surface nucleation and seeded growth method. The application of JPs in the biomedical field is explored such as drug delivery, bio-imaging and bio-sensing. The scheme is shown in Fig. 1. Finally, a summary for the design, preparation and biomedical applications of JPs are constructed, furthermore, we present an introduction to the current challenges faced by these materials with a perspective on future directions of development.

## 2. Design and preparation of Janus particles

### 2.1. Design of Janus particles

Janus particles as a class of materials, have a characteristic anisotropic structure, composition and properties and are considered as some of the most complicated colloidal particles in existence. Over the past few decades, related research has attracted considerable interest due to the

novel properties and unique applications of JPs. However, fabrication of a desired shape, size, components, and additional parameters face big challenges, as translating the properties of the building blocks into the properties of overall materials and combining the different components together, requires a complex and smart design of synthetic routes. Toward this end, researchers have done a great deal of work to better design JPs. In the section, the design principles for JPs are highlighted, especially those relevant to biomedical applications, based on the morphology, particle size, and components of JPs.

#### 2.1.1. Morphology and particle size

There have been various shapes of JPs reported in many articles, including dumbbell [23,55], rod [56], snowman [25,57], or any of a variety of other shapes [3,6]. It is well recognized that properties and applications of JPs are highly dependent on their morphology and chemical composition. JPs with nano-/micro-objects not only offer complex morphologies and asymmetry but can combine individual components together without losing the intrinsic optical, magnetic, and electronic properties [58].

Due to the heterojunction of different components, Janus nanoparticles can integrate components of different and opposite character and can simultaneously display the properties and characteristics of both materials. These properties and materials can be altered depending on purpose. For example, the Janus design enables the combination of two opposing properties, hydrophobicity and hydrophilicity [59] or other physicochemical properties [60], into single particle that can be used in a variety of fields. Among these is the creation of amphiphilic Janus structure, which is designed by tuning the hydrophilic and hydrophobic domains of the JPs, akin to control hydrophilic-lipophilic balance (HLB) of traditional organic surfactants. Thus, the produced materials may be exploited as both surfactants and catalysts [61,62]. Liu and yang et al. [23] successfully constructed dumbbell-shaped amphiphilic JPs, containing one hydrophobic and one hydrophilic sphere, can act as interface-active solid catalysts to stabilize Pickering emulsions. And the Janus catalyst exhibited better catalytic performance than commercial Pt/C catalyst in aqueous hydrogenation reactions, as shown in Fig. 2A. Recently, Zhao et al. [63] designed the dual-mesoporous  $\text{Fe}_3\text{O}_4@m\text{-C} & m\text{-SiO}_2$  ( $m$ -being the notation for mesoporous) Janus nanoparticles, containing a pure one-dimensional mesoporous  $\text{SiO}_2$  nanorod and a closely connected mesoporous  $\text{Fe}_3\text{O}_4@m\text{-C}$  magnetic nanosphere. Through adjusting the volume ratio between the hydrophilic and hydrophobic domains in single Janus nanoparticle, endows the Janus nanoparticles with a surfactant-like ability for emulsion

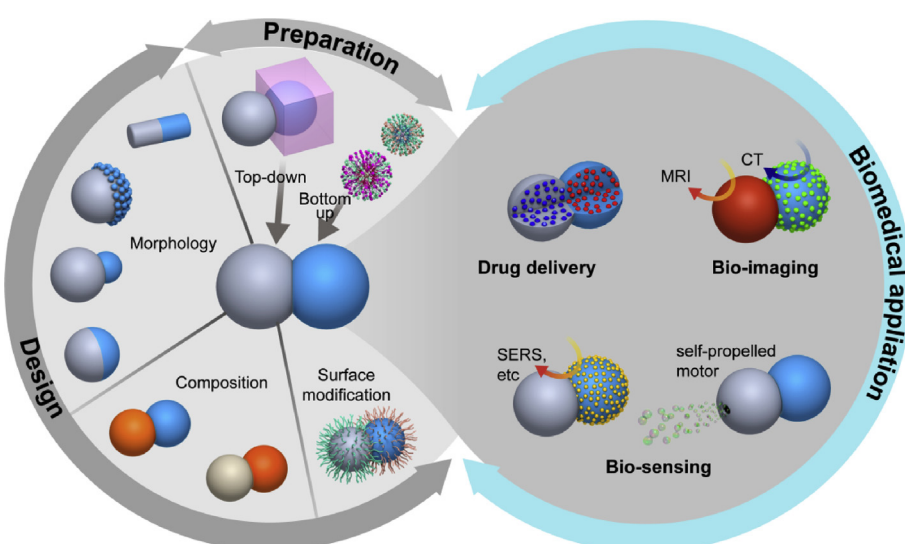
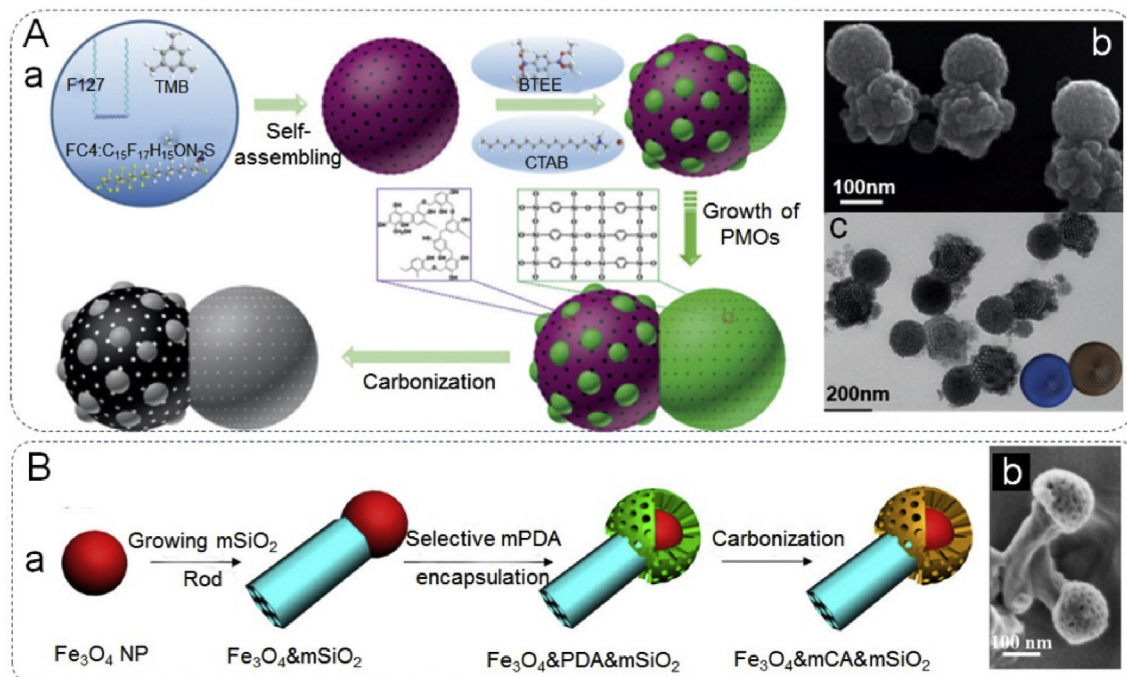


Fig. 1. Schematic illustration of the design, preparation, and biomedical application of Janus particles.



**Fig. 2.** The amphiphilicity of the Janus particles. (Aa) Graphic illustration of the synthesis of the Janus nanoparticles, (Ab) SEM image and (Ac) TEM image of the as-synthesized Janus RF&PMO nanoparticles. Reproduced with permission from Ref. [23]. Copyright 2017, Wiley-VCH. (Ba) Fabrication scheme of Fe<sub>3</sub>O<sub>4</sub>@mC&mSiO<sub>2</sub> Janus nanoparticles, (Bb) SEM image of Fe<sub>3</sub>O<sub>4</sub>@mC&mSiO<sub>2</sub>. Reproduced with permission from Ref. [63]. Copyright 2018, American Chemical Society.

stabilization, while also allowing for magnetic separation and recycling both of these features are crucial for improving the efficiency of biphasic catalysis (Fig. 2B). Furthermore, unique optical properties and extraordinary catalytic properties can be obtained through combining components possessing surface plasmon resonance or excellent catalytic properties such as noble metals [64–66]. The unique morphology of Janus nanoparticles is also well suited for the combination of magnetically active materials, resulting in significantly enhanced separation character following drug delivery, biocatalytic uses and bio-imaging [67–69]. Moreover, Janus particles have been increasingly documented in their efficacious ability to stabilize immiscible polymer mixtures. Although heterogeneous materials developed for this purpose are not new, they suffer from preferential wetting, due to the low interfacial tensions (ITs) involved. This is because particles will only adsorb to an A-B interface only if it has a greater interfacial tension than the difference between that experienced by the particles with each of the components,  $IT_{A-B} > |IT_{P-A}-IT_{P-B}|$ . If this is not satisfied, the particles preferentially adsorb to one of the phases and fail to serve their intended purpose [70]. However, Janus particles overcome this problem by presenting two materials, each more suited to one or the other of the biphasic components, while being physically connected; preventing preferential wetting and making interfacial adsorption between the two phases more preferable for the system. Although Janus particles tailored in this way offer great advantages over existing media, their complex synthetic process has slowed research. Despite this, there have been numerous reports of Janus materials being synthesized and used as compatibilizing agents [3, 70–73]. The development of Janus materials is highly applicable to biomedical applications as the capability of tailoring two sets of characteristics within the same particle offers myriad opportunities that have yet to be fully explored. When considering the problems faced by the drug delivery field, the bipartisan nature of Janus particles could hold the key to allowing the co-delivery of both hydrophobic and hydrophilic drugs or drugs with dissimilar solubility [73]. However, a more specialist use of this morphology is simultaneous imaging and treatment. An example of this is seen in Xu et al.'s work concerning the use of an antibody functionalized Au-Fe<sub>2</sub>O<sub>3</sub> dumbbell particles that offered

enhanced imaging capabilities while also benefiting from the magnetic properties to provide magnetolytic therapy [74,75].

Further to the impressive degree of control over the JPs morphology and the tailorabile chemical and physical properties, research has proven that this control extends to overall particle size, as well. Most published studies document particle sizes that range from a few hundred nanometers to a few micrometers. However, reports on the synthesis of much smaller nano-sized (< 100 nm) JPs present a greater challenge and are actually rather scarce [60]. As the inherently complex, and simplest, morphology of JPs consists of two building blocks, its size tends to fall into the submicrometer range. A variety of methods have been reported for the preparation of (sub) micron-sized JPs. In the preparation of submicrometer JPs of polyacrylonitrile (PAN) and polystyrene (PS) via a one-step batch seeded emulsion polymerization (Fig. 3A). Both the high degree of cross-linking and the slow feeding of the monomer were crucial to control the resultant anisotropic structure [76]. In the synthesis, an example submicrometer crosslinked polyacrylonitrile (PAN) hollow colloid was used as a seed, a monomer mixture of styrene/divinylbenzene (St/DVB) was slowly added into the seed emulsion at high temperature to allow for polymerization. Synthetic methods towards JPs have been the focus of significant research. Most methods are lengthy and complex, owing in part to the complexity of the final structure. However, despite these challenges, many nanoscale Janus structures and synthetic techniques have been reported. For example, Schick et al. [27] fabricated monodisperse multifunctional and highly biocompatible Au@MnO JPs by a seed-mediated nucleation and growth technique that produced JPs of about 25 nm size (Fig. 3B). The metal oxide domain could be coated selectively with a thin silica layer, leaving the metal domain untouched. In particular, size and morphology of the individual (metal and metal oxide) domains could be controlled by adjustment of the synthetic parameters.

### 2.1.2. Composition

The dual nature of Janus nanoparticles allow for novel and complicated architectures, not only of size and morphology, but composition as well. It is of vital importance to understand the relationship between the

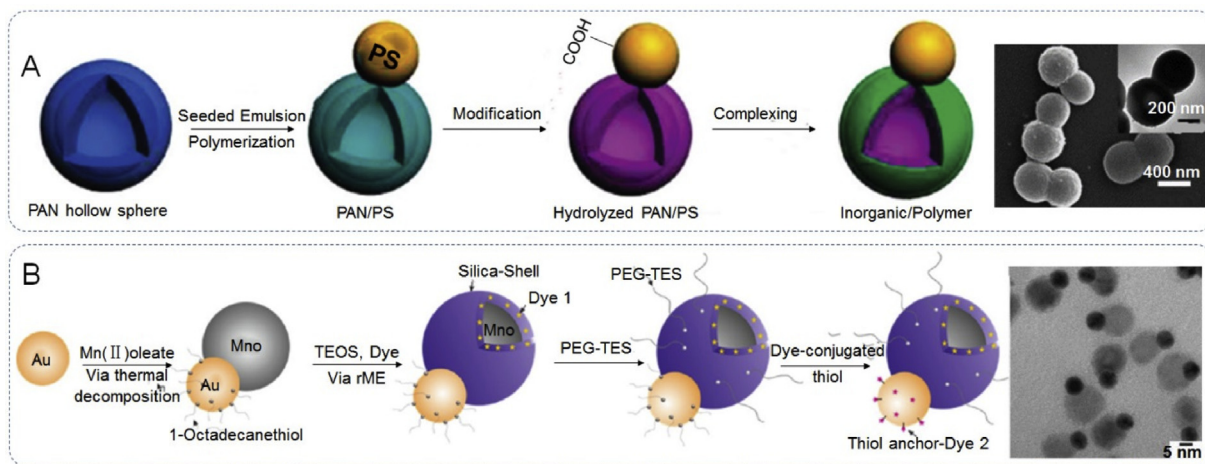


**Fig. 3.** The size of the Janus particles. (A) The synthesis of submicrometer Janus PAN/PS colloids and electron image. Reproduced with permission from Ref. [76]. Copyright 2010, American Chemical Society. (B) The synthesis of nanoscale ( $< 100$  nm) Janus Au@MnO heterodimers and SEM image. Reproduced with permission from Ref. [27]. Copyright 2014, American Chemical Society.

components of the colloidal building blocks and the potential value of single particles. In recent years, significant effort has been devoted to developing JPs with diverse components, reporting considerable progress towards this goal. This section describes recent studies on a variety of component designs of JPs, which can be generally grouped into three categories: polymeric, inorganic, and polymeric-inorganic. Following this, an individual discussion of each category with a number of select representative works from the most recent literature will be presented.

#### 2.1.2.1. Polymeric Janus particles.

Polymeric JPs have attracted extensive attention from both industrial and academic areas because of the soft

nature of the polymer backbone and the easily tailored asymmetric structure, which allows controllable physicochemical properties; their application areas range from medicine, biochemistry and physics to colloidal chemistry [6,77]. Recently, various well established strategies have been reported for the successful fabrication of polymeric JPs, typically including phase separation, self-assembly, and microfluidic strategies. Recently, the phase separation method was demonstrated in a work by Ku et al., where they reported the synthesis of pH-responsive biphasic JPs consisting of polystyrene/poly(2-vinylpyridine) (PS/P2VP) homopolymers. Subject to the geometry and pH-dependent hydrophilic–lipophilic balance, the newly synthesized PS/P2VP JPs were also

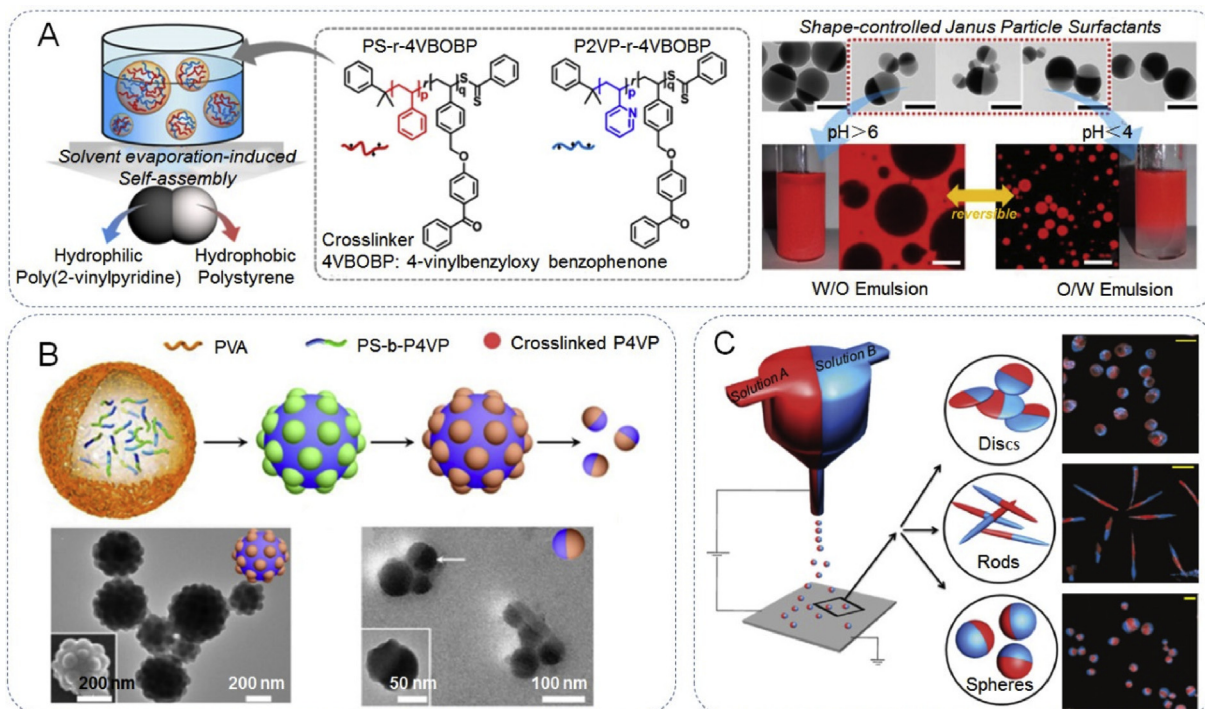


**Fig. 4.** Fabrication of Janus nanoarchitectures with polymeric components. (A) Schematic illustration of the preparation of amphiphilic PS/P2VP Janus particles and a facile transformation of emulsion types achieved by adjusting the pH of the aqueous phase (bottom). Reproduced with permission from Ref. [78]. Copyright 2017, American Chemical Society. (B) Self-assembly of diblock copolymer polystyrene b-poly(4-vinylpyridine) (PS-b-P4VP) by an emulsion solvent evaporation method for the synthesis of patchy Janus particles with P4VP protuberances on their surface. Reproduced with permission from Ref. [79]. Copyright 2015, American Chemical Society. (C) Fabrication of biodegradable bicompartimental spherical, discoid, and rod-shaped microparticles via an electrohydrodynamic co-jetting of poly(lactide-co-glycolide) (PLGA) polymer solutions. Reproduced with permission from Ref. [80]. Copyright 2010, Wiley-VCH.

able to control the reversible formation, breakage, and switching of Pickering emulsions. Moreover, the switchable behavior and the associated stabilization of the emulsions at different pH could also be regulated by varying the relative ratio between PS and P2VP (Fig. 4A) [78]. Self-assembly from diblock copolymer has also been approved to be very convenient to fabricate different types of polymeric Janus nanostructures. In a typical example, Deng et al. [79] presented the self-assembly of a diblock copolymer, polystyrene-b-poly(4-vinylpyridine) (PS-b-P4VP), by an emulsion solvent evaporation method to synthesize patchy JPs with P4VP protuberances on their surface (Fig. 4B), which are amphiphilic and of self-organization into superstructures. The ratio of P4VP/PS and thus, the Janus balance of the NPs, can be tunable by changing the block chain length ratio of the block copolymers. Within the P4VP domains, other species, including metallic and inorganic, are favorably grown to achieve the respective functional composite Janus NPs. In addition to the previously mentioned phase separation or self-assembly, microfluidic synthesis and electrodynamic co-jetting of polymer solutions have also attracted great attention in recent years [6,77]. The design of these co-jetting microfluidic synthesis methods can be tuned by controlling the various parameters of the polymer solutions, such as concentration, viscosity, and conductivity. Polymer JPs with different shapes, compositions, and compartmentalization can be achieved via this method. Fig. 4C shows work by Bhaskar et al. concerning the fabrication of biodegradable bicompartimental spherical, discoid, and rod-shaped microparticles via an electro-hydrodynamic co-jetting of poly(lactide-co-glycolide) PLGA polymer solutions from organic solvents through the control of concentration and flow rate of the two PLGA jetting solutions [80].

**2.1.2.2. Inorganic Janus particles.** Inorganic JPs can be divided into two types: the first type is JPs containing two or more different inorganic components phases. The other type involves a single inorganic phase with a different surface or other physical/chemical properties. These have shown great potential in magnetic, optical, and catalytic

applications [6]. Like those documented for polymeric JPs, the fabrication of inorganic JPs has also received extensive attention. Examples of the typical synthesis methods for inorganic JPs include surface controlled nucleation, immobilization method and metal evaporation, though there are many others [8,39].

In the reported literature, the composition of inorganic JPs is mostly common inorganic composition, such as silica, metal, metal oxide, etc. For example, Zhao et al. [81] constructed a multifunctional diblock and triblock mesoporous silica-based Janus nanocomposites, which contained a 1D mesoporous organosilicate nanorod and a closely connected dense  $\text{SiO}_2$  nanosphere located on one side of the nanorods, (Fig. 5A). Furthermore, the triblock mesoporous silica nanocomposites composed of a cubic mesostructured nanocube, a nanosphere with radial mesopores and a hexagonal mesostructured nanorod that can also be fabricated with the anisotropic growth of mesopores. The obtained asymmetric  $\text{Au-NR@SiO}_2\&\text{EPMO}$  mesoporous nanorods with ultrahigh surface area, unique 1D mesochannels and functional asymmetry can be used as an ideal nanocarrier for the controlled release of drug molecules using a near-infrared, photothermal trigger. Several articles have reported the deposition of  $\text{SiO}_2$  or metallic oxide onto gold nanorods. Silica ( $\text{SiO}_2$ ) is of special interest for deposition in patches on inorganic NPs, such as,  $\text{SiO}_2$  lobes on the Au nanorods. Rowe et al. [82] reported a method for controlling the morphology of  $\text{SiO}_2$ -overcoated gold nanorods ( $\text{SiO}_2\text{-GNRs}$ ). The  $\text{SiO}_2$  shell uniformly coats whole GNRs or forms lobes on the ends of the Au nano-bipyramids depending on the concentration of tetraethoxysilane (TEOS) in the TEOS/ methanol (MeOH) solvent. The size of the  $\text{SiO}_2$  lobes can be controlled, but there is a minimum lobe size, below which full encapsulation is favored (Fig. 5B). Zhang et al. [83] reported a facile wet-chemistry route that selectively coats crystalline ceria on the Au nanorods (Fig. 5C). These nanostructures can be achieved with the assistance of bifunctional potassium tetrachloroplatinate(II) ( $\text{K}_2\text{PtCl}_4$ ), which can selectively adsorb on both ends of the Au NRs to trigger the autoredox reaction of the ceria precursor. The unique structure is favorable for the adsorption and activation of  $\text{N}_2$  molecules due to the

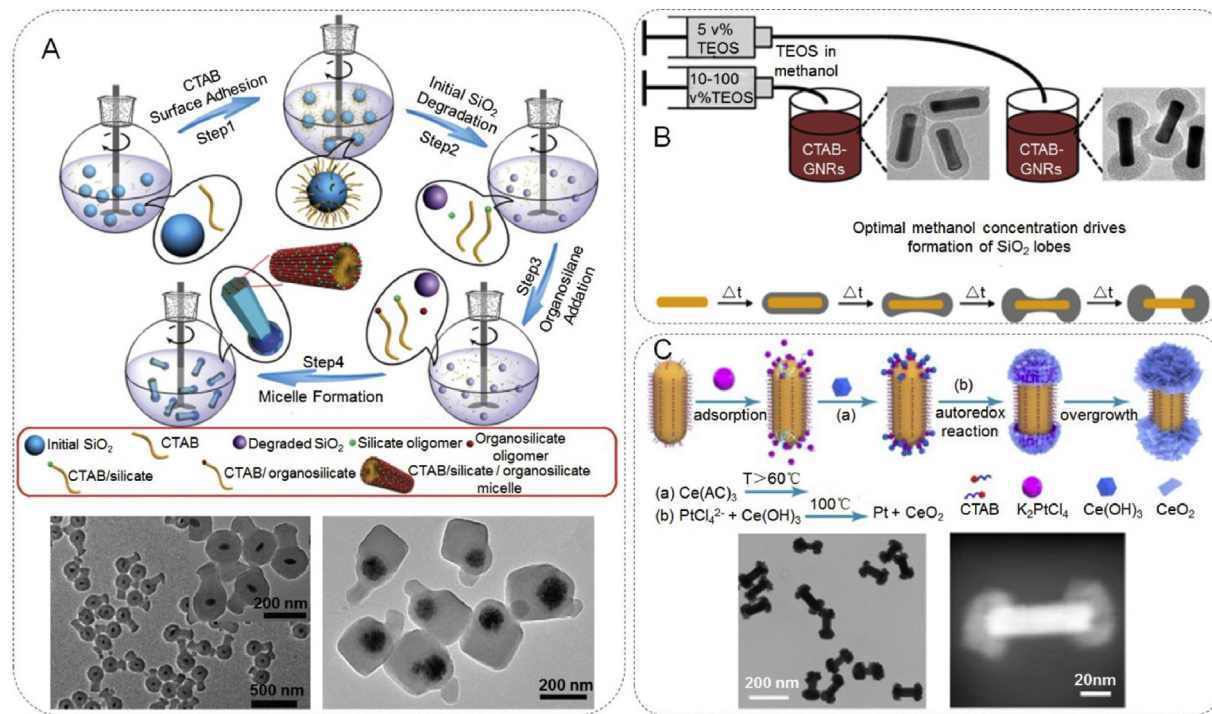


**Fig. 5.** Fabrication of Janus nanoarchitectures with inorganic components. (A) Schematic illustration of degradation-restructuring induced anisotropic epitaxial growth for the synthesis of asymmetric diblock nanocomposites and TEM image. Reproduced with permission from Ref. [81]. Copyright 2017, Wiley-VCH. (B) Cartoon depicting proposed mechanism of lobe formation facilitated by MeOH. Reproduced with permission from Ref. [82]. Copyright 2018, American Chemical Society. (C) Schematic illustration of the synthesis process of Au/end-CeO<sub>2</sub> nanostructure and electron image. Reproduced with permission from Ref. [83]. Copyright 2019, American Chemical Society.

oxygen vacancy (OVs) rich surface of grown ceria. The obtained Au/end-CeO<sub>2</sub> are an excellent catalyst for nitrogen photofixation under near-infrared (NIR) illumination. Beyond the above-mentioned inorganic Janus composites, Janus nanostructures have also been studied with other components, such as Au-TiO<sub>2</sub>, Au-ZnO, Au-Fe<sub>3</sub>O<sub>4</sub>, Pt-Au Janus nanowire, etc.

**2.1.2.3. Polymeric-inorganic Janus particles.** Compared with polymeric and inorganic JPs individually, polymeric-inorganic JPs combine both the easy processing, flexibility and even environmentally responsive properties of organic components and the mechanical, magnetic, and photoelectric properties of inorganic counterparts [6]. For polymeric-inorganic JPs, the most widely used synthesis techniques are: emulsion polymerization, confined nucleation and growth and immobilization. Nagao et al. prepared monodisperse dumbbell-shaped hybrid Janus structures through a surfactant-free emulsion polymerization technique (Fig. 6A). This method consists of three steps of double surfactant-free emulsion polymerizations that take place before and after a heterocoagulation. In the first step, a surfactant-free emulsion polymerization covers the silica cores with cross-linked poly (methyl methacrylate) (PMMA) shells. Then, positively or negatively charged silica nanoparticles were heterocoagulated with the silica-PMMA core-shell particles. In the third step, surfactant-free polymerizations at different pH values were performed to produce a polystyrene bulge from the core-shell particles, supporting the charged silica nanoparticles [84]. Through a competing growth, the composite structure of inorganic silica and a resorcinol-formaldehyde (RF) resin Janus material has been reported (Fig. 6B) [85]. The Janus dendritic mesoporous silica (DMS)@RF nanoparticle displays a bonsai-like morphology which consists of a

dendritic mesoporous silica unit and an RF sphere unit. Through tuning the polymerization rates of silica and RF, eccentric and concentric core-shell nanostructures have been successfully prepared. Notably, some heterogeneous hybrid Janus nanostructures have also been synthesized, such as Fe<sub>3</sub>O<sub>4</sub>-PS, ZnO-PS, PS-Fe<sub>3</sub>O<sub>4</sub>, PS-SiO<sub>2</sub>, SiO<sub>2</sub>-polymer, etc. [39].

### 2.1.3. Surface modification

Exploring the design of JPs, asymmetric surface chemistry can be obtained through the surface modification of isotropic particles. A common synthetic theme in surface modification is to protect part of the initial isotropic particles while selectively functionalizing of particles in the unprotected part of the area, (i.e. anisotropic *part area* over the whole *particle surface*). The theme often involves a masking step, where particles are temporarily trapped at the interface between two phases, such as a liquid–liquid or liquid–solid interface, exposing the two sides of a particle to different chemical environments [77]. This technique allows for the treatment of a specified portion of the particles' surface, which lead to the formation of these complex structures.

With this strategy, the Janus particles are symmetric in shape but asymmetric in surface properties, due to the distribution of different functional groups over the particle surfaces. For example, the use of planar surfaces to mask a part of the particle surface has been used to synthesize metal/polystyrene and metal/silica JPs [65,86,87]. Maspoch et al. [88] made advances towards a general protecting strategy to synthesize porous metallic Janus metal-organic framework (MOF) particles, based on depositing MOF particles onto a planar surface, followed by the direct evaporation of metal components on the surface of the colloidal MOF crystals that had been exposed (Fig. 7A). Deng et al. [89] reported

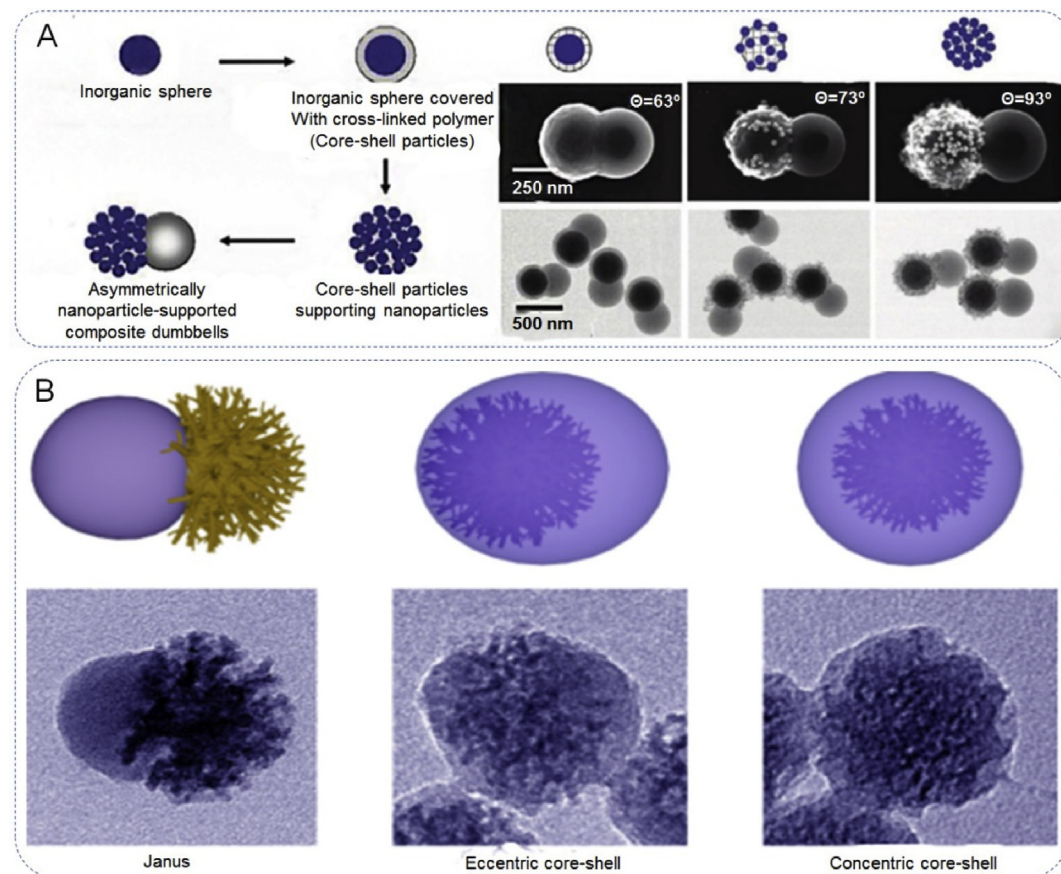


**Fig. 6.** Fabrication of Janus nanoarchitectures with polymeric-inorganic hybrid components. (A) Preparation of dumbbell-like asymmetrically polymeric-inorganic hybrid nanoparticle by grafting growth. Reproduced with permission from Ref. [84]. Copyright 2011, American Chemical Society. (B) Fabrication of dendritic mesoporous silica@resorcinol-formaldehyde (DMS-RF) Janus nanostructure via a competing growth mechanism. Reproduced with permission from Ref. [85]. Copyright 2017, American Chemical Society.

the fabrication of Janus polystyrene (PS) microspheres that were partially covered with ZnO nanowires (Fig. 7B). The area for ZnO growth on a microsphere can be tailored by varying the thickness of the polymer mask. The PS microspheres with carboxylate groups were immersed in an aqueous solution of ZnCl<sub>2</sub>. This treatment of the microspheres beforehand with Zn<sup>2+</sup> effectively improved the growth of ZnO nanowires on the microspheres. The conductivity of the polymer mask was also an important factor for obtaining uniformly distributed ZnO nanowires on the microspheres.

Surface modification can also be explained in other ways. Subsequent to the synthesis of JPs, these nanoparticles can be engineered and functionalized by incorporating different functional groups located at surfaces or through the modification of existing ligand. This allows for the inclusion of more complex and novel features to an unprecedented degree. For this purpose, Liu et al. [57] reported that the water-wettability

of ionic liquids (ILs) can be used in the modification of JPs to easily incorporate new functionalities through a simple anion exchange (Fig. 7C). In this methodology, two different ionic liquids were added on opposite sides is unstable, the anions would easily exchange in the solvent. Therefore, the water-wettability of the particles was tuned by anion exchange of the ILs, which provided a facile functionalization of the snowman-like JPs. To design multifunctional nanoparticles, Zhang et al. [90] designed an elaborate multifunctional Au/Fe<sub>3</sub>O<sub>4</sub>@C Janus nanoparticles (JNPs), which underwent further selectively functionalized functionalization with amino-poly(ethylene glycol)thiol (NH<sub>2</sub>-PEG-SH) (Fig. 7D). Their anisotropic surface properties and various functionalities, allow them to house several components for the detection and targeting of cancer cells.

On the whole, Janus particles can be functionalized in several different ways. One way involves the self-assembly of ABC triblock

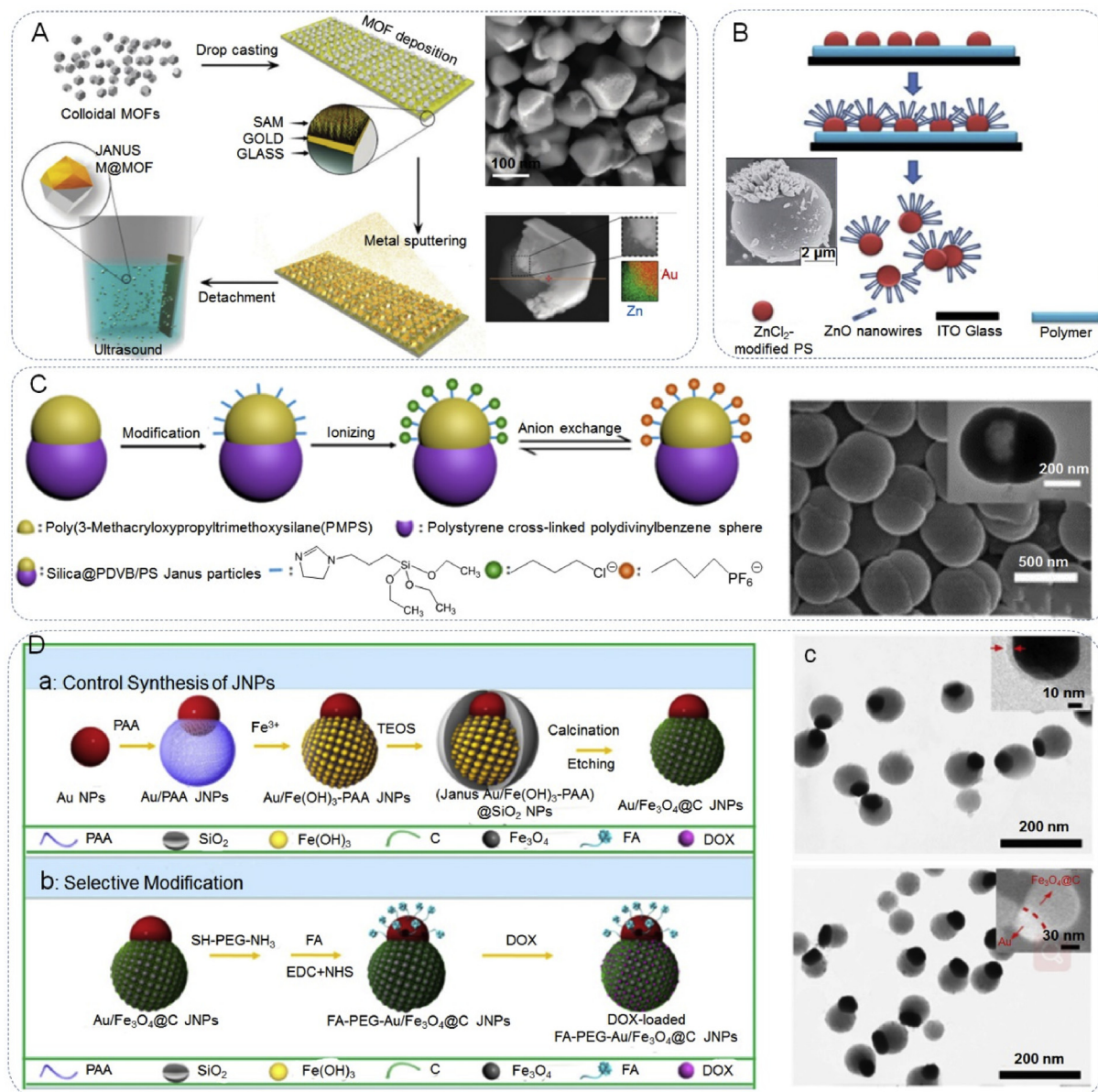


**Fig. 7.** Design of Janus particles by Surface modification. (A) Synthesis of metallic Janus MOFs via the desymmetrization at interfaces approach and SEM image. Reproduced with permission from Ref. [88]. Copyright 2016, Royal Society of Chemistry. (B) Formation of Janus PS microspheres with ZnO nanowires by masking and electrochemical methods and SEM image. Reproduced with permission from Ref. [89]. Copyright 2010, Royal Society of Chemistry. (C) Illustration of the synthesis of ionic liquids modified Janus particles and the anion exchange process. Reproduced with permission from Ref. [57]. Copyright 2019, American Chemical Society. (Da) Schematic showing the controlled synthetic strategy for obtaining Au/Fe<sub>3</sub>O<sub>4</sub>@C JNPs, (Db) selective modification of Au/Fe<sub>3</sub>O<sub>4</sub>@C JNPs, (Dc) electron images of Janus Au/Fe(OH)<sub>3</sub>-PAA@SiO<sub>2</sub> NPs and Au/Fe<sub>3</sub>O<sub>4</sub>@C JNPs. Reproduced with permission from Ref. [90]. Copyright 2017, Wiley-VCH.

polymers into particles consisting of the “B” chain, while the “A” and “C” sections remain accessible as surface functionalization [6,73]. Through careful manipulation of the functional group density in the polymers, it is possible to tune the amount of surface functionalization [91]. Another method is through the incorporation of appropriately functionalized monomers into the bulk of the particles to form handles on the surface of the particle, following curing. In this way, amino groups were successfully introduced to one hemisphere of the particle body, that was applied towards the binding of biotin to the particle surface [92]. Another work detailed the production of Janus materials using a seeded dispersion polymerization induced phase separation to leave only the desired

functional groups in two distinct areas on the particle surface while maintaining spherical structure [93]. The functional monomers were not incorporated into the main sphere, but instead polymerized around solid polystyrene spheres in a highly controllable manner, allowing for the precise tailoring of surface functionality.

## 2.2. Synthetic method of Janus particles

Over the past few decades, various strategies have been reported for the successful synthesis of Janus materials, including: phase separation, self-assembly, surface nucleation and seeded growth, toposelective

**Table 1**  
Typical Janus fabrication methods, compositions, particle size, and morphologies.

Fabrication methods	Compositions	Morphologies	Schematic	Size	Ref
Phase separation	PS-P2VP	Dumbbell		Nanoparticles	[78]
	PtBA/PS	Hamburger,		Nanoparticles	[95]
	PLLA/PS	Spherical		Nanoparticles	[96]
Immobilization	SiO <sub>2</sub> -Au	Spherical		Nanoparticles	[87]
	SiO <sub>2</sub> -PS	Snowman		Nanoparticles	[97]
	ZnO-PS	Irregular		Microparticles	[89]
Surface-controlled nucleation and growth	silica@RF	Bonsai-like		Nanoparticles	[85]
	Au-SiO <sub>2</sub>	Octopus-type		Nanoparticles	[17]
	Au-Fe <sub>3</sub> O <sub>4</sub>	Dumbbell		Nanoparticles	[98]
Self-assembly	PS-PI-PMMA	Irregular		Nanoparticles	[99]
	PS-b-P4VP	Raspberry		Nanoparticles	[79]
	PS-b-P4VP	Irregular		Nanoparticles	[100]
Microfluidics	Poly(lactide-co-glycolide)	Discoid, rod, Spherical		Microparticles	[80]
	PNIPAAm-SPO-fluorophore-PMBA	Snowman		Microparticles	[101]
	PNIPA-SPO	Snowman		Microparticles	[102]
Emulsion polymerization	SiO <sub>2</sub> -polymer	Core-shell-corona		Nanoparticles	[103]
	PVDF/P(St-co-tBA)	Raspberry		Nanoparticles	[104]
	TPGDA/DMS	Snowman		Microparticles	[105]

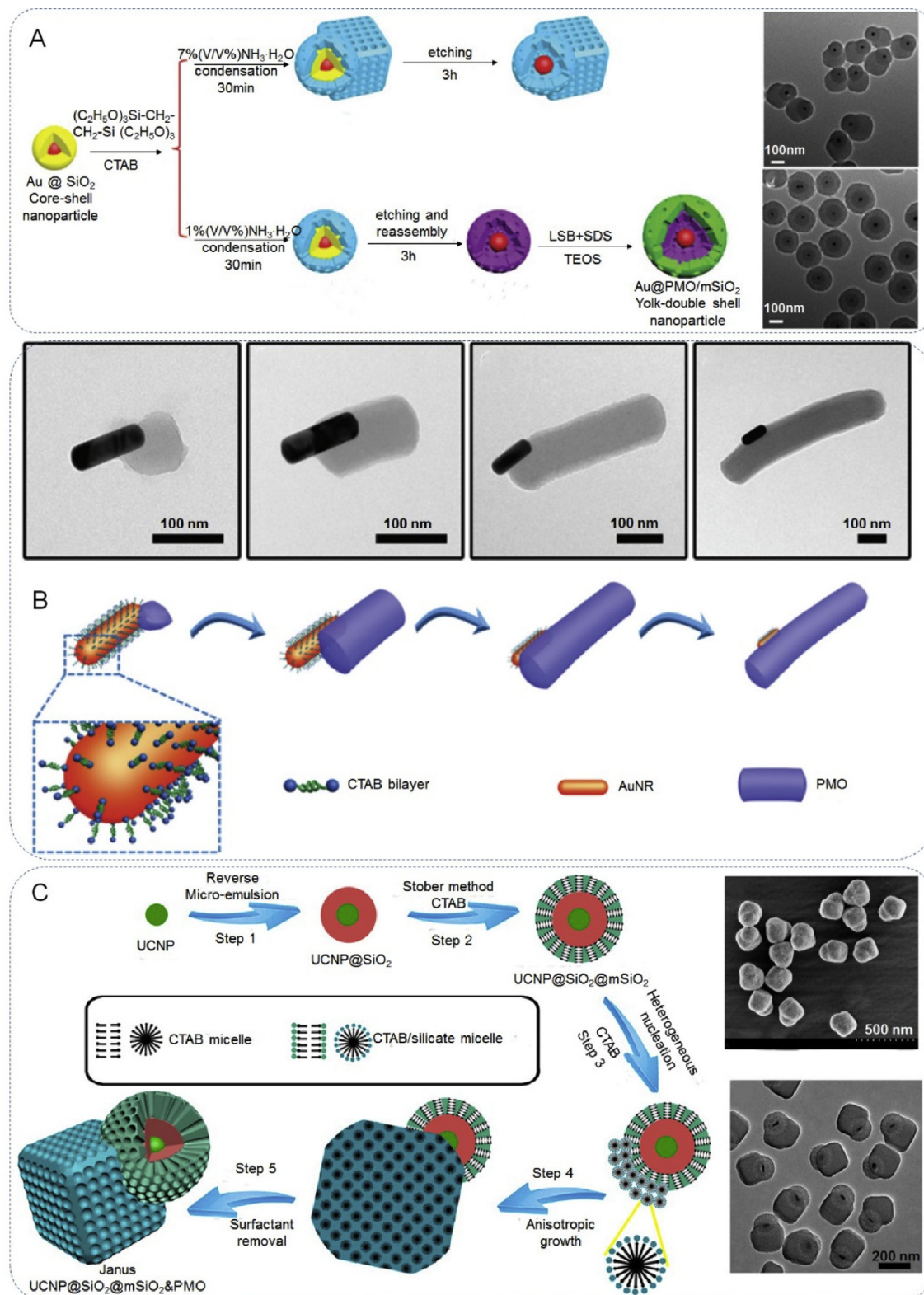


**Fig. 8.** The construction of Janus particles by surface nucleation and seeded growth method. (A) The synthesis illustration of Au&PMO Janus, Au@PMO yolk-shell, and Au@PMO/mSiO<sub>2</sub> yolk-double shell nanostructures. Reproduced with permission from Ref. [108]. Copyright 2016, Royal Society of Chemistry. (B) TEM images of single nanoparticle obtained at different reaction times and schematic illustration of the formation of rod-like Janus AuNR@PMO nanoparticles. Reproduced with permission from Ref. [109]. Copyright 2017, Royal Society of Chemistry. (C) Synthesis of UCNP@SiO<sub>2</sub>@mSiO<sub>2</sub>&PMO Janus mesoporous silica nanocomposites by an anisotropic island nucleation and growth method. Reproduced with permission from Ref. [47]. Copyright 2014, American Chemical Society.

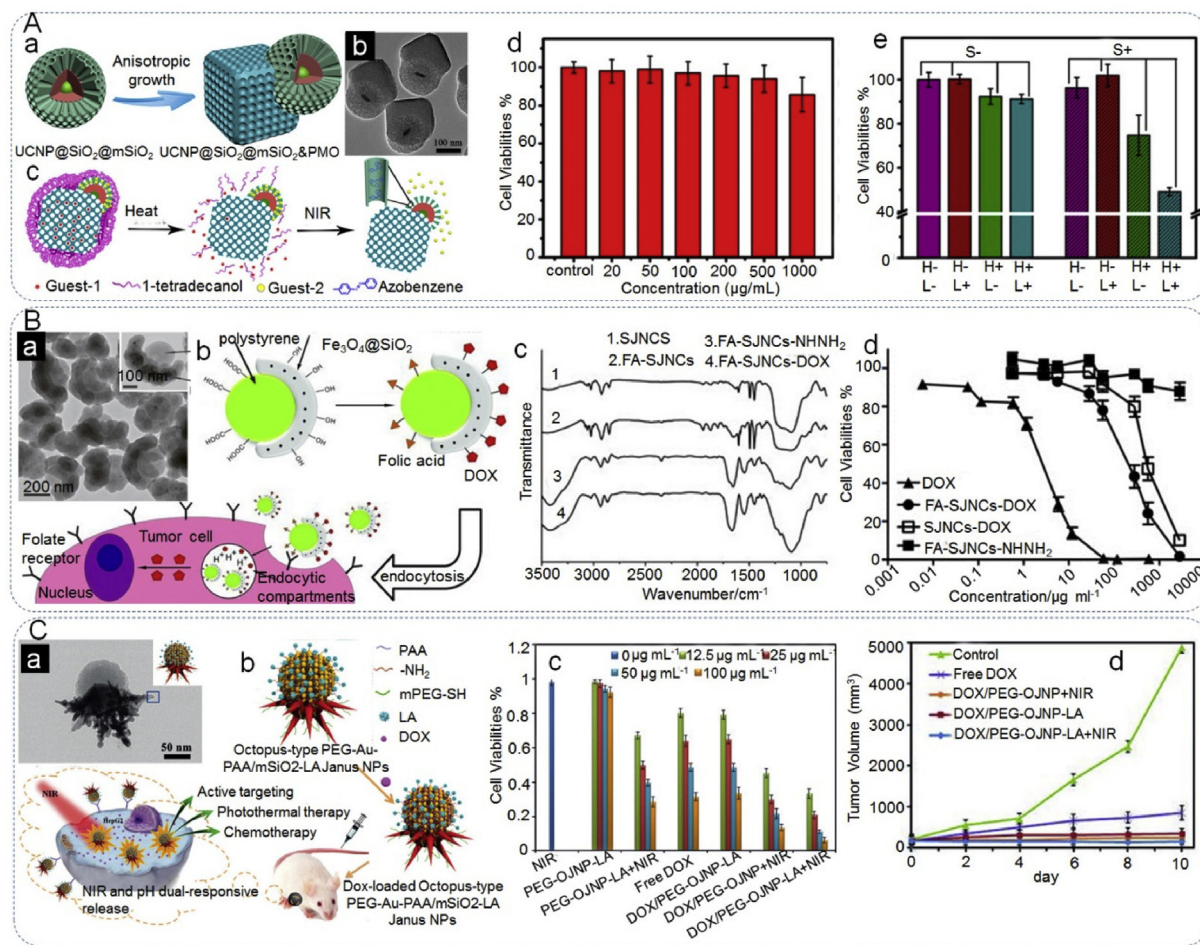


**Fig. 9.** Janus particles as drug carriers for drug delivery. (Aa) Schematic illustration of the synthesis of UCNPs@SiO<sub>2</sub>@mSiO<sub>2</sub>&PMO particles, (Ab) TEM image of UCNPs@SiO<sub>2</sub>@mSiO<sub>2</sub>&PMO Janus nanocomposites, (Ac) schematic presentation for dual control drug release systems by using the dual compartment mesoporous Janus nanocomposites, (Ad) MTT cell viability assay of Janus UCNPs@SiO<sub>2</sub>@mSiO<sub>2</sub>&PMO nanocomposites on HeLa cells, (Ae) cell viabilities of paclitaxel and DOX co-loaded UCNPs@SiO<sub>2</sub>@mSiO<sub>2</sub>-Azo&PMO-PCM Janus nanocomposites under the heat (H) and NIR light (L) treatment (S means sample). Reproduced with permission from Ref. [47]. Copyright 2014, American Chemical Society. (Ba) TEM image of SJNCs (the SJNS image at higher magnification), (Bb) schematic diagram illustrating the proposed mechanisms for tumor cell targeting and stimulus-induced drug release, (Bc) FTIR spectra of 1) SJNCs, 2) FA-SJNCs, 3) FA-SJNCs-NHHN<sub>2</sub>, and 4) FA-SJNCs-DOX, (Bd) in-vitro cytotoxicity profiles of DOX, FA targeted SJNCs-DOX conjugates, non-targeted SJNCs-DOX conjugates, and drug-free control SJNCs using human MDA-MB-231 breast cancer cells. Reproduced with permission from Ref. [4]. Copyright 2013, Wiley-VCH. (Ca) HRTEM image of a single PEG-OJNP-LA, (Cb) schematic illustration of pH and NIR light dual-stimuli responsive properties for actively targeted and chemo-photothermal cancer therapy in vitro and *in vivo*, (Cc) MTT cell viability assay of HepG2 cancer cells with different treatments, (Cd) relative tumor volume from the H-22-tumor-bearing Kunming mice with different treatment. Reproduced with permission from Ref. [17]. Copyright 2016, Wiley-VCH.

surface modification (immobilization), microfluidics, Pickering emulsions interfacial synthesis, etc. [6,39,94] Not surprisingly, many reviews have summarized the synthesis methods of Janus. In order to provide a different outlook, we will summarize the synthesis methods of Janus used in recent years and highlight the most common methods. Table 1 summarizes the typical fabrication methods, compositions, particle size and morphologies of a number of representative Janus structures.

Of all the methods, surface nucleation and seeded growth is the most prevalent method for the construction of JPs, especially for the complex morphologies. The anisotropic growth of JPs is affected by the total surface energy change function, which can be represented by equation (1):

$$\Delta\sigma = \sigma_{1-2} + \sigma_{2-s} - \sigma_{1-s} \quad (1)$$

Where  $\Delta\sigma$  refers to total Gibbs free energy change,  $\sigma_{1-2}$  represents the interfacial energy between the initial nuclear component (1) and second component (2),  $\sigma_{2-s}$  and  $\sigma_{1-s}$  are the surface energies of the two components in solvent [106,107]. According to this equation, the JPs grow homogeneously or heterogeneously depending on the energy barrier on

the surface of the system. If the variation in the total surface is positive, the system induces the formation of the asymmetrical structure. On the contrary, if  $\Delta\sigma$  is negative, component (2) isotropically coats on the component (1) surface to form a symmetrical structure. For this purpose, by adjusting the reaction parameters (temperature, surfactant, solvent), the growth mode of the system can be changed from Frank-van der Merwe mode to a Volmer-Webber mode, resulting in the formation of Janus nanostructures instead of core-shell structures [47,107]. Through a competing growth, a novel Au & periodic mesoporous organosilica (PMO) Janus nanostructure has been prepared (Fig. 8A) [108]. In this method, Au&PMO Janus, Au@PMO yolk-shell and Au@PMO/m-SiO<sub>2</sub> yolk-double shell nanoparticles, can be obtained by using Au@SiO<sub>2</sub> nanoparticles as seeds and using NH<sub>3</sub>H<sub>2</sub>O as the basic catalyst and etching agent. Through controlled nucleation and growth, Zhang et al. [109] reported a monodisperse rod-like Janus AuNR@PMO nanostructures with precisely controlled morphology, such as fingernail- and horsebean-like structures (Fig. 8B). In the synthesis, the seed-shape of PMO was determined by the shape of Au nanoparticles. Adjusting the system environment (temperature, surfactant, solvent), caused further

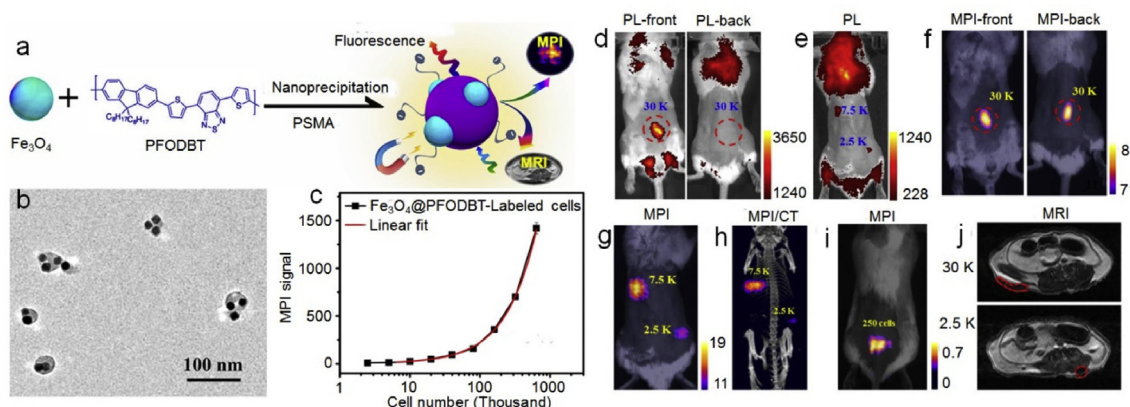


**Fig. 10.** Janus particles as contrast agents for bio-imaging. (a) Schematic of the preparation of  $\text{Fe}_3\text{O}_4@\text{PFODBT-COOH}$  Janus nanoparticles through nanoprecipitation, (b) TEM image of  $\text{Fe}_3\text{O}_4@\text{PFODBT-COOH}$  Janus nanoparticles, (c) plot of MPI signals vs. the number of  $\text{Fe}_3\text{O}_4@\text{PFODBT-COOH}$  labeled cells, (d, e) fluorescence imaging of a mouse from front or back view after local subcutaneous injection of  $\text{Fe}_3\text{O}_4@\text{PFODBT-COOH}$  labeled cells, (f, g) two-dimensional projection MP imaging of mouse from front view or back view, after local subcutaneous injection of labeled cells, (h) three-dimensional MPI and CT imaging of mouse after local subcutaneous injection of labeled cells, (i) overlay of white light picture and 2-D projection MPI image of a mouse implanted 250 labeled cells after background subtraction, (j) MRI transverse images of mouse body after local subcutaneous injection of cells labeled with  $\text{Fe}_3\text{O}_4@\text{PFODBT-COOH}$ . Reproduced with permission from Ref. [145]. Copyright 2017, American Chemical Society.

polymerization of the organosilica to grow on the nucleation site that had been formed beforehand through the classical Volmer-Weber island growth mode, resulting in the formation of a variety of shaped AuNR@PMO Janus nanostructures, rather than the core-shell nanostructure. Using a novel anisotropic island nucleation and growth approach, shown in Fig. 8C, Zhao et al. [47] successfully synthesized dual-compartment Janus *m*-silica nanocomposites UCN-P@ $\text{SiO}_2@m\text{SiO}_2\&\text{PMO}$  (UCNP referred to upconversion nanoparticle, NaGd-F4:Yb,Tm@NaGdF4) and UCN@ $\text{SiO}_2@m\text{SiO}_2@\text{PMO}$  nanoparticles, by varying the volume ratio between  $\text{H}_2\text{O}$  and ethanol in the synthesis mixture. In the typical synthesis, core@shell UCN@ $\text{SiO}_2$  nanoparticles was first prepared as seeds, and then used with two different silanes as the precursors for the formation of the different domains of the heterodimer JPs. The synthesis strategy of anisotropic growth-induction may open new directions to construct complex Janus nanostructures with tailored properties [17,110].

Furthermore, Janus particle synthesis is often reliant upon the differences in surface tension between the would-be particles and surrounding solvent in order to form certain shapes [73]. In fact, the exploitation of surface tensions between the solid nanoparticles, “soft” polymer droplets and the liquid solvent is most often used to form asymmetric particle shapes [111–114]. The asymmetric nature occurs during the synthesis because as the interfacial tensions between this tri-phasic system increases with the maturity of the polymerization reaction, the solid nanoparticle and polymer surface begin to dewet [112], thus form asymmetric particles rather than spheres as a core@shell system.

### 3. Janus particles in biomedical applications

#### 3.1. Janus particles for drug delivery

In the field of drug delivery, materials like mesoporous silica (or carbon) nanoparticles [115–119], core-shell nanoparticles [120–122], hollow structured nanoparticles [123–125], have been widely used as drug carriers for cancer therapy in research. However, it is challenging to realize combined therapy with loading multidrugs on these materials, due to their symmetrical structure and limited storage space. Even when multidrugs are simultaneously loaded in the storage space, drugs with different chemical properties (e. g., hydrophilicity/hydrophobicity, acidity/basicity, etc.) will react with each other and the independent release of each drug is almost impossible to control [4]. In contrast, JPs

are composed of two or more compartments that are anisotropic in nature. This makes them ideally suited for multidrug loading or modification with diverse functional molecules for separate drug release [47,48,126–130], or cancer therapy [4,17,131–134].

The intensive research of these materials as drug carriers is due to their anisotropic properties [15,18,48,135], and selectable drug release triggers like: pH [14,15], temperature [136], light [137] or two of them [17,18,47,48]. For example, Li et al. [47] fabricated Janus mesoporous silica nanocomposites (UCNP@ $\text{SiO}_2@m\text{SiO}_2\&\text{PMO}$ ) composed of distinguished domains of hydrophilic composites (UCN-P@ $\text{SiO}_2@m\text{SiO}_2\&\text{PMO}$ ) and the hydrophobic component (PMO) (Fig. 9A). The hydrophobic paclitaxel and hydrophilic doxorubicin (DOX) were used as model drugs, which were successfully loaded in the independent mesopores of the JPs, due to the anisotropic composition. Furthermore, the release of each drug was triggered independently by heat and NIR light, following modification with azobenzene (Azo) (light sensitive) and 1-tetradecanol (heat sensitive). The dual-drug loaded JPs achieved higher cancer cell destruction efficiency (more than 50%) than that of the single-triggered drug delivery system (~25%). Similarly, Zhang et al. [48] designed poly(3-caprolactone)-gold nanocage/ferric hydroxide-poly(acrylic acid) (designated “PCL-AuNC/Fe(OH)<sub>3</sub>-PAA”) JPs, with two distinct domains for the loading of hydrophilic doxorubicin (DOX) and hydrophobic drug, docetaxel. The drug loaded PCL-AuNC-/Fe(OH)<sub>3</sub>-PAA JNPs displayed enhanced tumor inhibition over the individual drugs. Wang et al. [4] synthesized Janus nanocomposites (SJNCs) of polystyrene/ $\text{Fe}_3\text{O}_4@\text{SiO}_2$ , composed of a PS core and a half silica shell with iron oxide nanoparticles embedded in its matrix (Fig. 9B). The PS and  $\text{Fe}_3\text{O}_4@\text{SiO}_2$  surfaces were functionalized with carboxyl and hydroxyl groups, respectively. The PS surface was modified with folic acid (FA) for the recognition of cancer cells that overexpress folate receptors and the silica shell was used for the loading of anticancer drug DOX via a pH-sensitive hydrazone bond that controlled the drug release. The hydrazone bond would be stable during bloodstream circulation (pH 7.4), inducing the release of DOX after exposure to the acidic endosomal compartment (pH 4.5–6.5). Thus ensuring only tumor cells would be exposed to the high concentrations of DOX and reduce any side-effects, inducing significant cancer cell death.

Zhang et al. [17] constructed octopus-type PEG-Au-PAA/mSiO<sub>2</sub>-LA Janus NPs (PEG-OJNP-LA) by using Au@poly(acrylic acid) (PAA) JNPs as templates to grow a mesoporous silica (mSiO<sub>2</sub>) shell on the PAA unit and Au branches on the Au component, in addition to being separately modified with lactobionic acid (LA) for tumor-specific targeting and

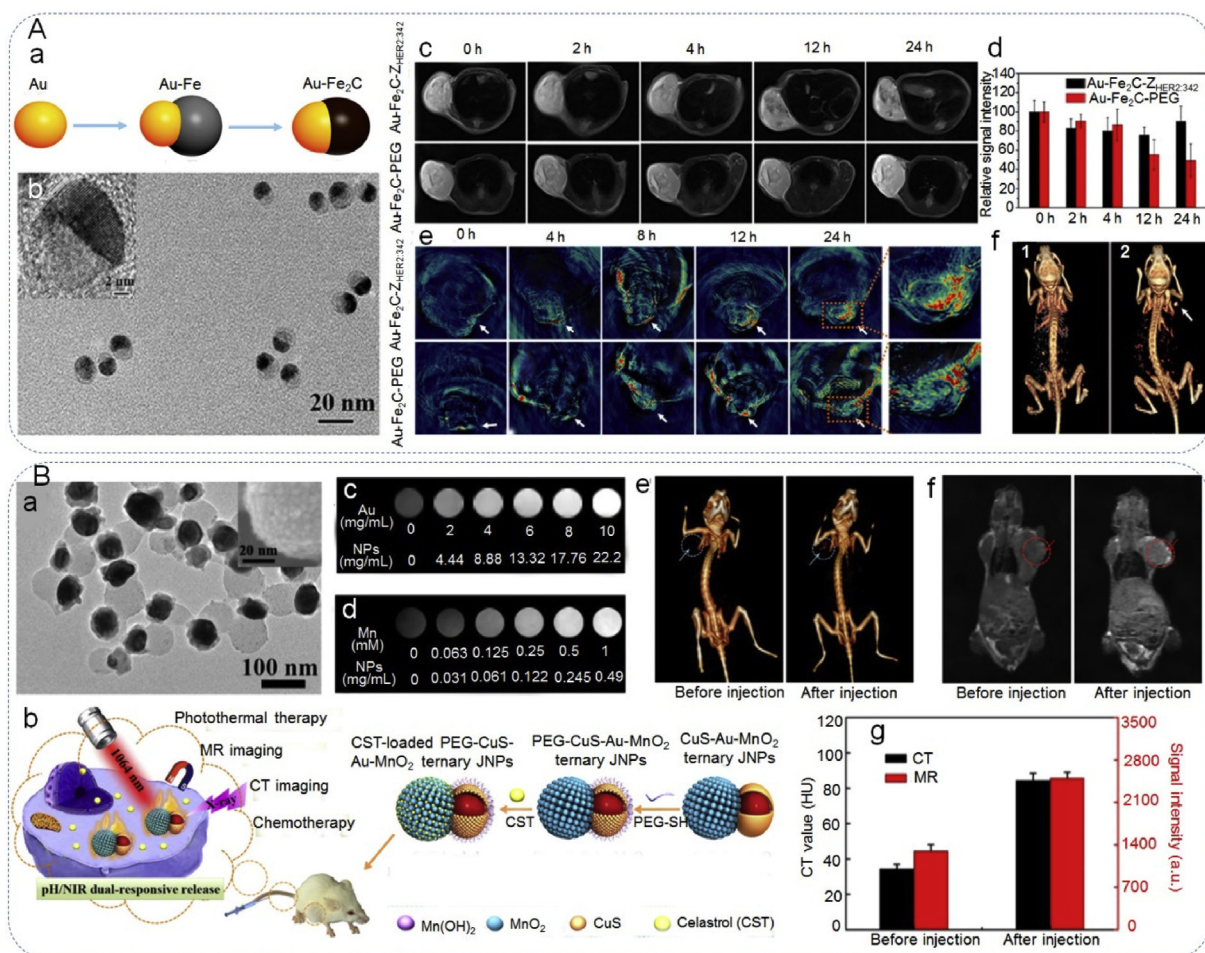


**Fig. 11.** Janus particles as contrast agents for bio-imaging. (Aa) Schematic illustration of the synthetic process of  $\text{Au}-\text{Fe}_2\text{C}$  JNPs, (Ab) TEM and HRTEM (inset) images of  $\text{Au}-\text{Fe}_2\text{C}$ -PEG JNPs, (Ac) real-time T2-weighted MR images of MDA-MB-231 tumor-bearing mice at various time points before and after intravenous injection of  $\text{Au}-\text{Fe}_2\text{C-Z}_{\text{HER}2:342}$  JNPs and  $\text{Au}-\text{Fe}_2\text{C}$ -PEG JNPs, (Ad) relative MR signal intensity in the tumor at different time points after administration of injection, (Ae) *in vivo* MSOT images of tumors in mice taken at different times after intravenous injection of  $\text{Au}-\text{Fe}_2\text{C-Z}_{\text{HER}2:342}$  JNPs and  $\text{Au}-\text{Fe}_2\text{C}$ -PEG JNPs, (Af) 3D reconstructed CT images before 1) and after the intratumor injection 2) of  $\text{Au}-\text{Fe}_2\text{C}$ -PEG JNPs. Reproduced with permission from Ref. [142]. Copyright 2017, American Chemical Society. (Ba) TEM image of PEG-CuS-Au-MnO<sub>2</sub> ternary JNPs (inset: SEM image of MnO<sub>2</sub> domain), (Bb) schematic illustration of the fabrication procedures of PEG-CuS-Au-MnO<sub>2</sub> ternary JNPs for CT/MR imaging-guided chemo-photothermal cancer therapy in NIR-II window, (Bc and Bd) CT images and T1-weighted MR images of PEG-CuS-Au-MnO<sub>2</sub> ternary JNPs with different concentrations solution, respectively, (Be and Bf) *in vivo* three-dimensional CT images and T1-weighted MR images of mice before and after injection with PEG-CuS-Au-MnO<sub>2</sub> ternary JNPs for 24 h, respectively, (Bg) quantified CT and MR signals of tumors from mice before and after injection for 24 h. Reproduced with permission from Ref. [5]. Copyright 2018, American Chemical Society.

methoxy-poly(ethylene glycol)-thiol (PEG) for improved stability (Fig. 9C). The synthesized PEG-OJNP-LA exhibited high loading efficiency for DOX and possessed pH and NIR dual response release properties. Furthermore, DOX-loaded PEG-OJNP-LA presented higher toxicity at the cellular and animal levels than chemotherapy or photothermal therapy alone.

### 3.2. Janus particles for bio-imaging

Cell-based therapies (like cancer immunotherapy or stem-cell therapy), chemotherapy or photothermal therapy have received considerable attention in oncological research [138–140]. These therapeutic strategies often require imaging technologies to track the therapeutic cells or tissues in real time. OI, CT and MRI are commonly used imaging modalities, though these techniques are not without limitation. For example, OI presents poor spatial resolution and tissue attenuation [141]. CT and MRI are only efficient in detecting tumors larger than 0.5 cm and show low sensitivity [142,143]. Therefore, developing a nanoplatform to act as contrast agents for multi-imaging techniques would be highly beneficial for cell labeling and *in vivo* imaging. JPs that combine different functional

materials into a single unit, capable of diverse composition and surface chemistry, have been shown to exhibit excellent performance in multimodality imaging [27,50,144,145]. One such work by Schick et al. [27] synthesized  $\text{Au}@\text{MnO}@\text{SiO}_2$  JPs, which show great potential as a multifunctional platform for fluorescent tracking (fluorescent dye loading), MRI (MnO domain), and CT (AuNP face) imaging. Song et al. [145] constructed  $\text{Fe}_3\text{O}_4@\text{semiconducting polymer}$  JPs for cell tracking by multimodal imaging, especially magnetic particle imaging (MPI) (Fig. 10). MPI is a novel imaging modality that directly detects iron oxide nanoparticles by time-varying magnetic fields, rather than indirectly via MRI signal dropouts. This technique allows for high depth penetration, linear quantitation, low background, etc. compared with existing modalities. The authors synthesized iron oxide nanoparticles (IONPs) that exhibited higher MPI signals (effected by the size and crystal of IONPs) than the commonly used superparamagnetic iron oxide nanoparticles. These IONPs were then encapsulated with fluorescent semiconducting polymers to form  $\text{Fe}_3\text{O}_4@\text{semiconducting polymer}$  JPs, which simultaneously possessed optical and magnetic properties for MPI and fluorescence imaging. The results demonstrated that these JPs for MPI presented high sensitivity and unlimited tissue penetration towards *in vivo* cell

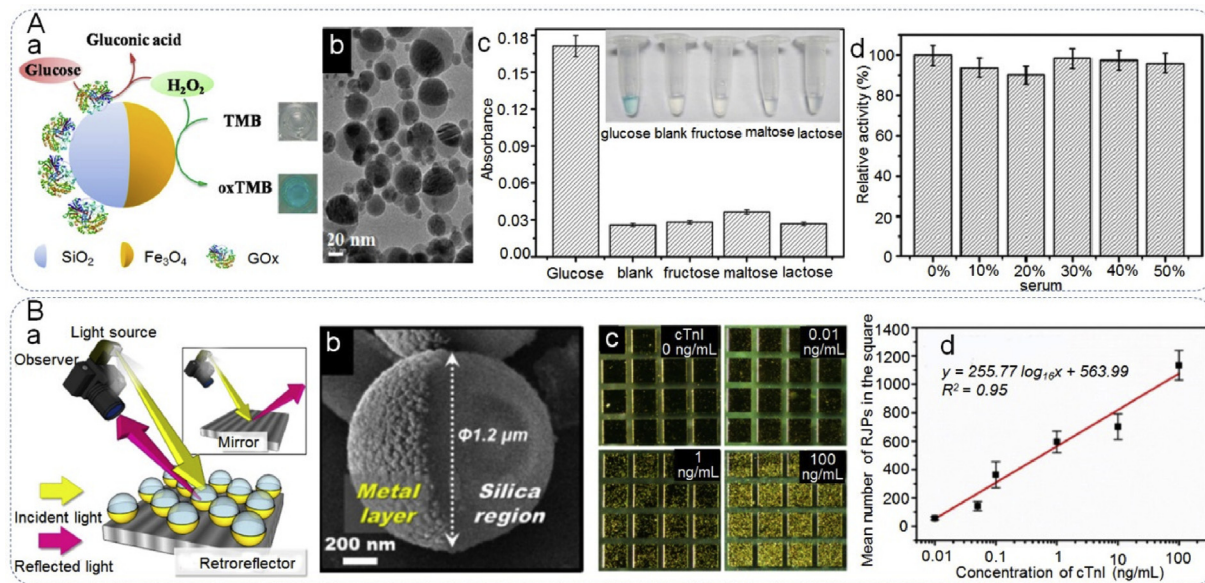


**Fig. 12.** Janus particles as biosensor for biomolecules detection. (Aa) Schematic illustration of the peroxidase-like activity of JFSNs in catalysis of the TMB-H<sub>2</sub>O<sub>2</sub> system and using GOx-JFSNs as biosensing platform for colorimetric detection of H<sub>2</sub>O<sub>2</sub> and glucose, (Ab) TEM image of JFSNs, (Ac) determination of the selectivity of glucose detection with glucose, no saccharide, fructose, lactose, maltose, and lactose (inset: photograph showing colorimetric responses of the system), (Ad) catalytic activity of glucose in buffer and in 10–50% fetal bovine serum. Reproduced with permission from Ref. [164]. Copyright 2015, American Chemical Society. (Ba) Schematic illustration of a typical light path in retroreflection, (Bb) SEM image of the isolated single RJP, (Bc) results of retroreflective cTnI immunoassay utilizing cTnI antibody-conjugated SMJPs, (Bd) dose-response curve for number of SMJPs in the square-pattered gold immunosensing zone as a function of cTnI concentration. Reproduced with permission from Ref. [33]. Copyright 2016, American Chemical Society.

tracking, compared with MRI and fluorescence imaging.

In addition to multiple imaging functions, JPs containing materials with strong ultraviolet (UV) or near-infrared (NIR) absorption are playing vital roles on imaging-guided phototherapy [142,146,147]. For instance, Ju et al. [142] successfully synthesized Au-Fe<sub>2</sub>C JNPs with broad absorption in the near-infrared range for photothermal therapy and multiple model imaging (Fig. 11A). Due to the special composition, Au-Fe<sub>2</sub>C JNPs were demonstrated to be excellent contrast agents for triple-modal MRI/multispectral photoacoustic tomography (MSOT)/CT imaging, which provided more integral information for precise diagnosis. Additionally, affibody protein (Z<sub>HER2:342</sub>) modified Au-Fe<sub>2</sub>C JNPs (Au-Fe<sub>2</sub>C-Z<sub>HER2:342</sub>) selectively targeted HER2 tumor cells and showed more accumulation and deeper penetration than non-targeting JNPs, resulting in the ablation of tumors without side-effects. The results indicated that Au-Fe<sub>2</sub>C-Z<sub>HER2:342</sub> had great potential as a multifunctional nanoplatform for efficient photothermal therapy as well as triple modal imaging in clinical situations.

Single-modality cancer treatments, such as photothermal therapy, chemotherapy, external radiotherapy, and radio frequency ablation, show limited efficacy and remain unsatisfying [131,148–150]. A combination of different therapies, therefore, is a facile method of synergistic treatment. The JPs can be designed with anisotropic materials composed of photosensitizers, radiosensitizers or a mesoporous structure for drug loading, while the previous section showed these materials can also serve as effective contrast agents. Recent studies have demonstrated that JPs can combine multiple therapeutic strategies and imaging capability for synergistic cancer therapy [5,49]. For example, Li et al. [5] designed ternary Janus nanoparticles composed of mesoporous MnO<sub>2</sub> at one side and an Au core covered with a CuS shell at the opposite side (designated as CuS-Au-MnO<sub>2</sub> ternary JNPs), towards imaging-guided synergistic chemothermal and photothermal therapy (Fig. 11B). MnO<sub>2</sub> segments can serve as drug carriers and MR imaging contrast agents. The Au domain showed strong X-ray absorption and is an ideal contrast agents for CT imaging. Meanwhile, the CuS shell presented strong absorption in the NIR, which is suitable for realizing photothermal conversion. After modification with PEG, CuS-Au-MnO<sub>2</sub> ternary JNPs demonstrated

excellent biocompatibility. Finally, celastrol (CST)-loaded PEG-Cu-S-Au-MnO<sub>2</sub> ternary JNPs exhibited high chemo-photothermal antitumor efficacy, both *in vitro* and *in vivo* under the guidance of CT/MR imaging.

### 3.3. Janus particles for bio-sensing

Biosensors that are capable of multiple functions, i.e. simultaneous detection of many diverse analytes and that also display separation, enrichment, signal transduction characteristics, have attracted increasing attention [151–156]. Considerable effort has been made to construct multiple nanostructures with multifunctional properties, such as core-shell particles [122,157–163]. However, additional coatings or modification will decrease these specialist properties. In contrast, the unique morphology of JPs make superior candidates for multifunctional biosensor construction. Recently, a variety of JNPs have been reported as biosensors for biomolecular detection [164,165]. For example, Lu et al. [164] fabricated a multifunctional biosensing platform composed of hematite-silica hybrid of Janus γ-Fe<sub>2</sub>O<sub>3</sub>/SiO<sub>2</sub> nanoparticles (JFSNs) for sensitive colorimetric detection of glucose (Fig. 12A). The JFSNs presented excellent peroxidase-like catalytic activity, due to the magnetic particle acting as a nanzyme that possesses an intrinsic peroxidase-like activity. Besides, the presence of SiO<sub>2</sub> facilitates the immobilization of glucose oxidase (GOx). Following which, the GOx-loaded JFSNs had both glucose oxidase-like and peroxidase-like activity. In one system containing tetramethylbenzidine (TMB), the material achieved fast, sensitive and colorimetric detection of glucose with high selectivity and reproducibility. Meanwhile, the biosensor exhibited an excellent capability for determination of glucose in serum. Su et al. [165] synthesized Janus PMO/Carbon spheres as a matrix of laser desorption/ionization mass spectrometry (LDI MS), which enhanced LDI MS detection of both hydrophobic and hydrophilic molecules due to its anisotropic properties. After loading silver particles, the JNPs simultaneously enabled direct diverse metabolites detection in serum without treatment beforehand, due to the selective LDI process caused by the nanoparticles. Other JNP materials have been used to construct immunoassay probes for macromolecule detection [33,51]. One such work by Han et al. [33]

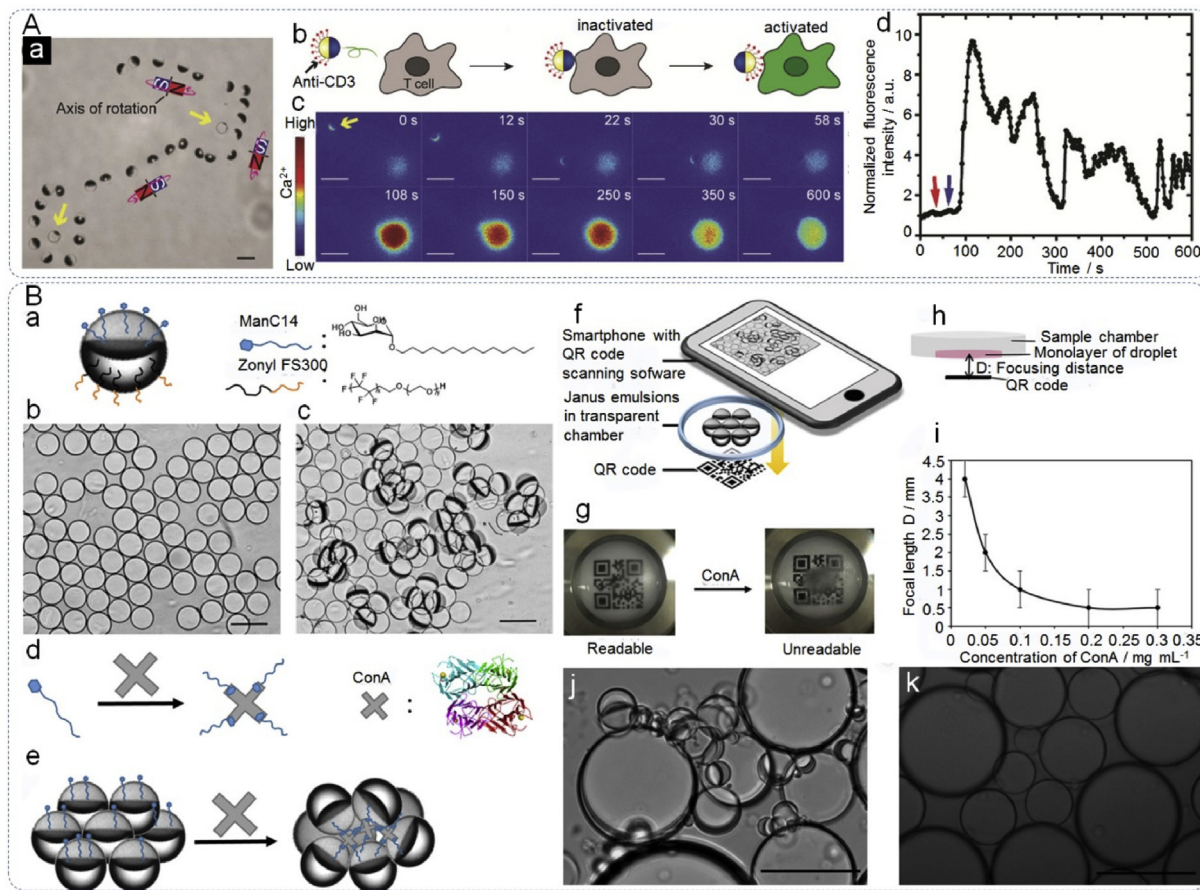


**Fig. 13.** Janus particles as biosensor for cell activation and bacteria detection. (Aa) Superimposed bright-field images showing that rotation and locomotion of a single Janus sphere can be simultaneously controlled to circumvent stationary particles (indicated by the yellow arrows) that were not magnetic responsive (scale bar 5  $\mu\text{m}$ ), (Ab) illustration showing the orientation of a Janus sphere and the corresponding T cell response, (Ac) fluorescence images showing T cell activation when the anti-CD3 coated hemisphere of a Janus sphere (indicated by the yellow arrow) was rotated to face the cell (scale bars 10  $\mu\text{m}$ ), (Ad) the normalized fluorescence intensity of the T cell shown in (Ab) is plotted against time to show the time dependence of T cell activation. Reproduced with permission from Ref. [52]. Copyright 2016, Wiley-VCH. (Ba) Side view of a Janus droplet stabilized by ManC14 and Zonyl FS 300, (Bb, Bc) optical micrographs of (Bb) transparent pristine monodisperse Janus emulsions and (Bc) agglutinated Janus emulsions scattering light after exposure to ConA (scale bar 100  $\mu\text{m}$ ), (Bd, Be) schematic representation of Janus emulsion agglutination: (Bd) multivalent binding of ConA to ManC14, (Be) agglutinated Janus emulsions with ConA and ManC14, (Bf) schematic view of qualitative detection of the agglutinated Janus emulsions, (Bg) optical signal detected using a QR code before and after exposure to ConA, (Bh) the focusing distance D, with droplet monolayer as a lens and QR code as the object, (Bi) correlation of the threshold ConA concentration for the binary signal with D, (Bj) Janus emulsion agglutination, 2 h after 4% paraformaldehyde treated ORN 178 *E. coli* bacteria were added, (Bk) no agglutination was observed with ORN 208 strains under the same testing conditions (scale bar equals 100  $\mu\text{m}$ ). Reproduced with permission from Ref. [16]. Copyright 2017, American Chemical Society.

synthesized retroreflective Janus microparticles (RJPs) for the analysis of cardiac troponin I (cTnI), an acute myocardial infarction (AMI)-specific biomarker (Fig. 12B). The RJP biosensor was designed by coating a highly reflective layer of Au on one hemisphere of silica particles. The Au hemisphere was subsequently modified with an antibody for the capture of cTnI. The retroreflection signals from RJPs were distinctively recognized as shining dots. As the concentration of cTnI increased as a result of the immune response, more shining dots were observed. On the basis of retroreflective immunosensing system, cTnI was detected with high sensitivity. Moreover, Sheng et al. [51] developed a magnetic encoded Janus microbead-based array with a gold “nanoisland” shell to enhance the fluorescence signals, making use of the local surface plasmon resonance (LSPR) properties of gold to achieve a highly sensitive multiplex immunoassay for various proteins.

Besides biomolecular analysis, JPs are playing vital roles for T cell activation [52,166] and bacteria detection [16]. T cell activation is an important step in immunotherapy, as activated T cells can recognize and attack cancer cells. However, most reported methods hardly realized control the signaling with single-cell precision [167,168]. To address this problem, Lee et al. [52] designed magnetic Janus microparticles to control of T-cell activation with the sought after single-cell precision

(Fig. 13A). The functional JPs were constructed by coating a thin magnetic nickel layer on one hemisphere and modifying an anti-CD3 antibody (that binds to the T cell receptor, triggering T-cell activation) on the silica hemisphere. Confirmation of T cell activation was quantified by measuring the concentration fluctuation of intracellular  $\text{Ca}^{2+}$  ions. Overall, the biosensing platform achieved remote control of single T cell activation by taking advantage of the unique magnetic response of JPs. Zhang et al. [16] reported Janus-based emulsion assays with carbohydrate-lectin binding for the detection of *Escherichia coli*, which can cause serious illnesses and even death (Fig. 13B). The Janus droplets would orient in a vertical direction as a result of the different densities of the two hemispheres. After the addition of *Escherichia coli* strains that express the mannose-specific lectin, the bacteria would bind to surface of the Janus droplets, which were modified with mannose, causing agglutination and a tilted geometry of the particles. The naturally aligned and agglutinated Janus droplets produced distinct optical signals, which can be detected quantitatively by a smartphone relying on the readable quick response (QR) code distance that varied with ConA concentration. The Janus emulsion assay offers simplistic preparation, long-term stability and exhibits high sensitivity and specificity for *Escherichia coli* detection. Compared with current methods for bacterial detection, like surface

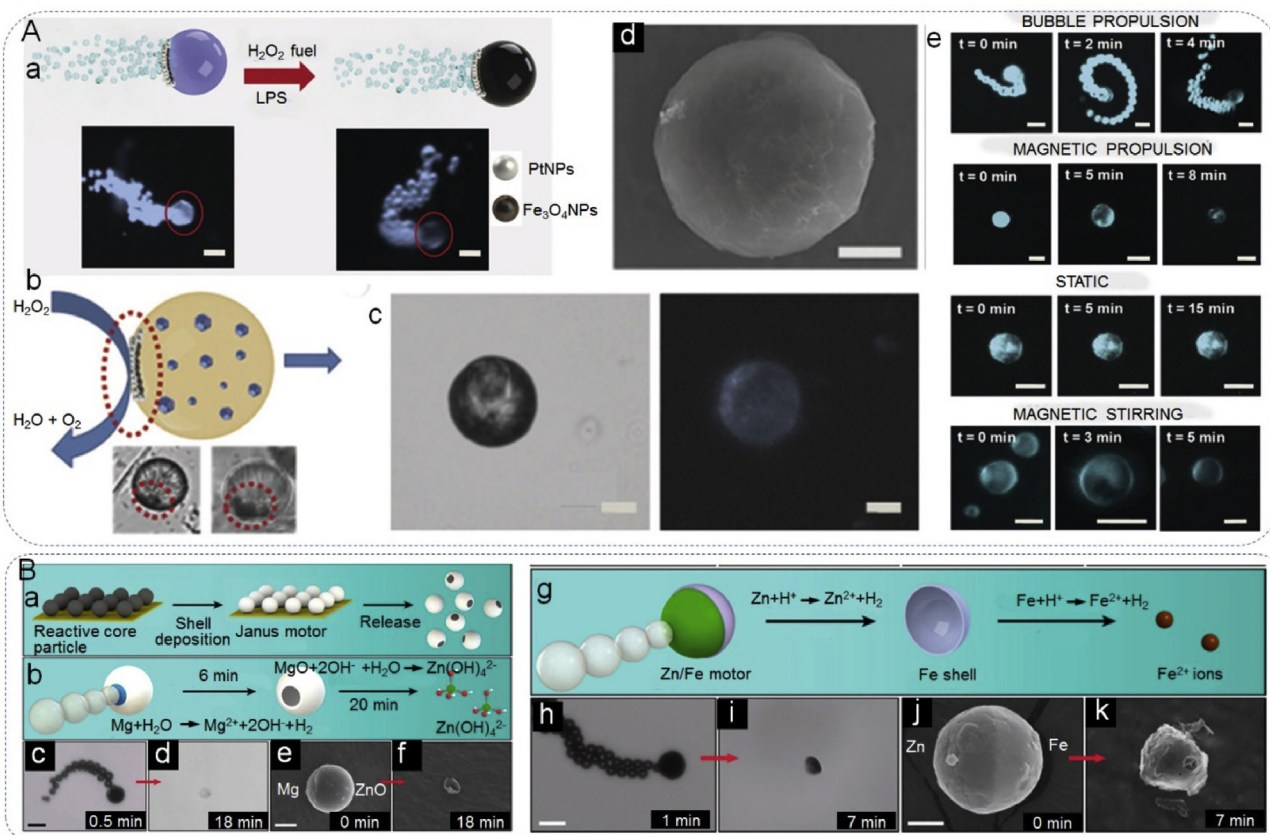


**Fig. 14.** Janus particles constructed self-propelled motors. (Aa) Bubble propulsion and optical microscopy images of the Janus micromotors before and after the addition of the lipopolysaccharide, (Ab) asymmetry and Janus character of the micromotors, (Ac) optical microscopy image showing the structure of the micromotors and corresponding fluorescence image, (Ad) SEM image of micromotors, (Ae) time-lapse microscopy images showing the fluorescence intensity of moving and static micromotors. Reproduced with permission from Ref. [53]. Copyright 2017, Wiley-VCH. (Ba) Fabrication of Janus micromotors: particles were spread on a glass substrate followed by sputtering of shell materials and release, (Bb) design of Mg/ZnO Janus micromotors, (Bc and Bd) microscope images of the propulsion and degradation of a typical Mg/ZnO Janus micromotor in 0.5 M NaHCO<sub>3</sub> solution at 0.5 and 18 min, respectively, (Be and Bf) SEM images of two typical Mg/ZnO Janus micromotors in 0.5 M NaHCO<sub>3</sub> solution at 0 min (unreacted) and 18 min, respectively, (Bg) design of Zn/Fe Janus micromotors, (Bh and Bi) microscope images of the propulsion and degradation of a typical Zn/Fe Janus micromotor in simulated gastric acid at 1 and 7 min, (Bj and Bk) SEM images of two typical Zn/Fe Janus micromotors at reaction times of 0 min (unreacted) and 7 min, respectively. Scale bars for Bc-Bf, Bh, Bi, 20  $\mu$ m; for Bj and Bk, 5  $\mu$ m. Reproduced with permission from Ref. [54]. Copyright 2016, American Chemical Society.

plasmon resonance (SPR), the polymerase chain reaction (PCR) and immunoassays, this biosensing assay is quicker, cheaper and portable.

JPs can be designed for pathogenic *Escherichia coli* bacteria capture and detection. In turn, non-pathogenic *Escherichia coli* has been used to apply JPs to the construction of self-propelled micromotors [169]. Nano- or micromotors are inspired by natural motility, such as the motion of sperm, bacteria, or molecular motors, and are promising materials in a plethora of biomedical applications; ranging from biomolecular detection to drug delivery and microsurgery [53,54,170, 171]. In comparison with other types of motors, JPs possess an anisotropic structure with distinct chemical or physical properties that allow for easy modification. Recently, many reports have showed that Janus micromotors exhibit excellent performance or great potential in biomedical applications [53,54,172,173]. For example, Jurado-Sánchez et al. [53] fabricated magnetocatalytic hybrid Janus micromotors encapsulating phenylboronic acid (PABA), that was in turn modified with graphene quantum dots (GQDs) for the detection of deadly bacteria endotoxins (Fig. 14A). The magnetic Fe<sub>3</sub>O<sub>4</sub> NPs and Pt NPs with intrinsic peroxidase-like activity, were loaded on one side of the Janus body. In the presence of hydrogen peroxide and a suitable magnetic field, the micromotor was able to actuate using bubble propulsion or magnetic actuation. PABA served as a highly specific receptor for the recognition of endotoxin. After the target endotoxin was captured, the

target interacted with GQDs that produced fluorescent quenching. The Janus micromotor displayed rapid and highly specific detection for deadly bacteria endotoxins, demonstrating considerable promise for more diverse clinical applications. Chen et al. [54] constructed self-destructing Mg/ZnO, Mg/Si, and Zn/Fe transient Janus micromotors that were able to autonomously disassemble in biological media after finishing their task (Fig. 14B). Magnesium (Mg), zinc (Zn), iron (Fe) and silicon (Si) are promising candidates for transient devices toward construction of self-destructible micromotors. Mg, Zn, and Fe are essential elements of human body and the final dissolved products are harmless to the *in vivo* surroundings. The Mg/ZnO, Mg/Si, and Zn/Fe Janus micromotors were driven by the bubbles produced by Mg-water, Zn-acid or Fe-acid reactions. The degradation of these materials relies on different corrosion rates of their core-shell components. The Mg- and Zn-based micromotors exhibited efficient bubble propulsion as well as controllable degradation rates. Further to this, the Zn-based micromotors showed high hemocompatibility and moved efficiently in biological fluid. These transient Janus micromotors offer considerable promise for diverse biomedical applications.

From the above cases, we conclude that JPs display remarkable performance in drug delivery, bio-imaging, and bio-sensing, suggesting great potential in constructing multifunctional systems for biomedical applications.

#### 4. Conclusion and outlook

This work explored the design strategies towards morphology, particle size, composition, and surface modification, which in turn affect the performance of JPs. Then, a review of the synthetic approaches for the preparation of JPs was conducted, highlighting surface nucleation and seeded growth method that appears to be the most popular method. Finally, we discussed the application of JPs in the biomedical field, including drug delivery, bio-imaging, and bio-sensing. Janus particles have attracted increased attentions for biomedical applications, exhibiting superior performance over existing technologies. Compared with isotropic polymer particles (like nano/microgels, hybrids etc.) or inorganic particles (like carbon, metals etc.), Janus particles are composed of two or more domains with anisotropic compositions and independent functions. Although individual components combine and coexist together in a single-particle system, the intrinsic physical and chemical properties of each domain are seldom altered or lost. So Janus particles as drug carriers can simultaneously realize multiple drugs (especially with opposite properties) loading and achieve synergistic therapeutic effect. If different domain is modified with pH/light/heat-sensitive molecules, the release of differential drugs can be separately controlled. Janus particles with optical/electrical/magnetic properties as contrast agents can be used for multimodal bio-imaging, combining with drug loading and realizing imaging-guided therapy. And Janus particles as biosensor can simultaneously detect many biomolecules, also can be used for the construction of self-propelled motors, achieving self-target drug delivery and cancer therapy.

On the whole, the novel anisotropic morphological structure has given Janus nanoparticles broad application prospects in many fields, not only biomedicine but also optics and catalysis. Despite these particles finding applications that allow them to begin to establish themselves, there are still considerable improvements to be made in terms of the currently manifested overly complex synthetic procedures and small scale production of Janus particles. Although various methods have been developed to synthesize Janus nanoparticles, more effort needs to be made towards simpler, larger scale production before these materials can be considered for industrial usage. The full realization of the potential these materials hold, cannot be explored before either of these problems has been solved as further applicational advancement is, while certainly within scientific interest, not a defining problem; in fact, the promise of these materials means that their tailored uses are myriad and their future, bright. From a materials science perspective, it is of the utmost importance to determine a set of theories and methods to direct and develop the synthesis of Janus particles. In this way, further research and iteration of existing methodology could provide the answers we seek, while allowing us to explore the novel physical and chemical properties that Janus materials are capable of offering.

Although JPs are playing irreplaceable roles in biomedical field, several major issues related biomedical applications still exist and require addressing. First, for drug delivery and bio-imaging *in vivo*, JPs retains the issues of biodegradability and toxicity. Developing Janus particles with biodegradable and low-toxic materials (Mg/ZnO etc.) that can dissolve harmlessly into their surroundings after completing any desired purpose, would represent a very powerful tool in this field. Besides, non-porous and non-spherical JPs often exhibit limited drug loading efficiency and poor therapeutic effect. Designing biocompatible JPs with porous or hollow structure is an important method to improve drug loading capacity. Meanwhile, constructing JPs that can simultaneously serve as contrast agents and drug carriers is a promising direction for realizing real-time monitoring and enhancing therapeutic effect. Moreover, Fabricating JPs composed of noble metal particles with catalytic activity exhibits a great potential in cancer therapy. Such as, Pt NPs possessing peroxidase-like activity can catalyze intratumoral H<sub>2</sub>O<sub>2</sub> to O<sub>2</sub> and enhance sonodynamic therapy. The JPs constructed by Pt as drug carrier, will realize synergistic therapeutic effect in cancer therapy. Second, although Janus motors especially powered by enzymes, serving

as biosensors present outstanding performance in biomolecules detection, drug delivery and targeted therapy, their performance may be compromised if faced biological media with complex components that will affect the speed of JPs. Moreover, it still remains a great challenge to simultaneously control the movement and direction of JPs. The fabrication of Janus motors by utilizing synergistic effect via combining enzyme catalytic reaction with an additional function such as light/thermal/magnetic has been developed for enhancing speed and controlling direction, which may be an important direction for the construction of next generation Janus motors. Third, it has been observed in many published papers that Janus particles present superior performance as drug carriers, contrast agents or biosensors compared with conventional uniform particles, however, little is known about the mechanism of how Janus particles work. With the rapidly increasing interest in these particles, it is necessary to understand the working mechanism of how the surface and structural anisotropy of JPs interact with the biological systems and affect biological functions. The fundamental understanding will drive the design of JPs, benefiting JPs' biomedical applications.

Briefly, from the design, preparation and biomedical applications, the morphology, particle size, composition, and surface modification will affect the JPs applications, and some well-controlled methods synthesized JPs present great performance in drug delivery, bio-imaging and bio-sensing compared to conventional uniform particles. Although fascinating advances on JPs biomedical applications have been witnessed. Some challenges still exist in developing simple and large-scale fabrication strategies, constructing biodegradable and low-toxic JPs with high drug loading capacity, designing JPs with both self-propelled and self-controlled properties as well as understanding the work mechanism of JPs. All the above undoubtedly have a long way from being addressed. Here, we hope that this review will provide better understanding of the design and preparation of JPs, while stimulating further interest in expanding the litany of biomedical applications.

#### Declaration of competing interest

We declare that we do not have any commercial or associative interest that represents a conflict of interest in connection with the work submitted.

#### Acknowledgment

We gratefully thank the financial support from Project 81771983, 81750410695, 81750110544, and 81851110764 by National Natural Science Foundation of China (NSFC), Project 16441909300 by Shanghai Science and Technology Commission, Project 2017YFC0909000 by Ministry of Science and Technology of China. This work is also sponsored by Shanghai Rising-Star Program (19QA1404800) and Innovation Research Plan supported by Shanghai Municipal Education Commission (ZXF082101). JL gratefully acknowledges the support of the Chinese Government 1000 Young Talent Plan.

#### References

- [1] P.G. de Gennes, Soft matter, *Science* 256 (5056) (1992) 495–497.
- [2] Y. Yi, L. Sanchez, Y. Gao, Y. Yu, Janus particles for biological imaging and sensing, *Analyst* 141 (12) (2016) 3526–3539.
- [3] A. Walther, A.H.E. Mueller, Janus particles: synthesis, self-assembly, physical properties, and applications, *Chem. Rev.* 113 (7) (2013) 5194–5261.
- [4] F. Wang, G.M. Pauletti, J.T. Wang, J.M. Zhang, R.C. Ewing, Y.L. Wang, D.L. Shi, Dual surface-functionalized janus nanocomposites of polystyrene/Fe<sub>3</sub>O<sub>4</sub>@SiO<sub>2</sub> for simultaneous tumor cell targeting and stimulus-induced drug release, *Adv. Mater.* 25 (25) (2013) 3485–3489.
- [5] S. Li, L. Zhang, X. Chen, T. Wang, Y. Zhao, L. Li, C. Wang, Selective growth synthesis of ternary janus nanoparticles for imaging-guided synergistic chemo- and photothermal therapy in the second NIR window, *ACS Appl. Mater. Interfaces* 10 (28) (2018) 24137–24148.
- [6] J. Hu, S. Zhou, Y. Sun, X. Fang, L. Wu, Fabrication, properties and applications of Janus particles, *Chem. Soc. Rev.* 41 (11) (2012) 4356–4378.

- [7] J. Du, R.K. O'Reilly, Anisotropic particles with patchy, multicompartiment and Janus architectures: preparation and application, *Chem. Soc. Rev.* 40 (5) (2011) 2402–2416.
- [8] C. Kaewsanhe, P. Tangboriboonrat, D. Polpanich, M. Eissa, A. Elaissari, Janus colloidal particles: preparation, properties, and biomedical applications, *ACS Appl. Mater. Interfaces* 5 (6) (2013) 1857–1869.
- [9] M. Lattuada, T.A. Hatton, Synthesis, properties and applications of Janus nanoparticles, *Nano Today* 6 (3) (2011) 286–308.
- [10] M.-J. Zhu, J.-B. Pan, Z.-Q. Wu, X.-Y. Gao, W. Zhao, X.-H. Xia, J.-J. Xu, H.-Y. Chen, Electrogenerated chemiluminescence imaging of electrocatalysis at a single Au-Pt janus nanoparticle, *Angew. Chem. Int. Ed.* 57 (15) (2018) 4010–4014.
- [11] X. Pang, C. Wan, M. Wang, Z. Lin, Strictly biphasic soft and hard janus structures: synthesis, properties, and applications, *Angew. Chem. Int. Ed.* 53 (22) (2014) 5524–5538.
- [12] P. Yanez-Sedeno, S. Campuzano, J.M. Pingarron, Janus particles for (bio)sensing, *Appl. Mater. Today* 9 (2017) 276–288.
- [13] S. Yue, X.T. Sun, N. Wang, Y.N. Wang, Y. Wang, Z.R. Xu, M.L. Chen, J.H. Wang, SERS-fluorescence dual-mode pH-sensing method based on janus microparticles, *ACS Appl. Mater. Interfaces* 9 (45) (2017) 39699–39707.
- [14] D. Shao, X. Zhang, W. Liu, F. Zhang, X. Zheng, P. Qiao, J. Li, W.-f. Dong, L. Chen, Janus silver-mesoporous silica nanocarriers for SERS traceable and pH-sensitive drug delivery in cancer therapy, *ACS Appl. Mater. Interfaces* 8 (7) (2016) 4303–4308.
- [15] D. Shao, J. Li, X. Zheng, Y. Pan, Z. Wang, M. Zhang, Q.-X. Chen, W.-F. Dong, L. Chen, Janus "nano-bullets" for magnetic targeting liver cancer chemotherapy, *Biomaterials* 100 (2016) 118–133.
- [16] Q. Zhang, S. Savagatrup, P. Kaplonek, P.H. Seeberger, T.M. Swager, Janus emulsions for the detection of bacteria, *ACS Cent. Sci.* 3 (4) (2017) 309–313.
- [17] L. Zhang, Y. Chen, Z. Li, L. Li, P. Saint-Criq, C. Li, J. Lin, C. Wang, Z. Su, J.I. Zink, Tailored synthesis of octopus-type janus nanoparticles for synergistic actively-targeted and chemo-photothermal therapy, *Angew. Chem. Int. Ed.* 55 (6) (2016) 2118–2121.
- [18] M. Zhang, L. Zhang, Y. Chen, L. Li, Z. Su, C. Wang, Precise synthesis of unique polydopamine/mesoporous calcium phosphate hollow Janus nanoparticles for imaging-guided chemo-photothermal synergistic therapy, *Chem. Sci.* 8 (12) (2017) 8067–8077.
- [19] Y.J. Zhao, Y. Cheng, L.R. Shang, J. Wang, Z.Y. Xie, Z.Z. Gu, Microfluidic synthesis of barcode particles for multiplex assays, *Small* 11 (2) (2015) 151–174.
- [20] Y. Wu, T. Si, J. Shao, Z. Wu, Q. He, Near-infrared light-driven Janus capsule motors: fabrication, propulsion, and simulation, *Nano Research* 9 (12) (2016) 3747–3756.
- [21] X. Ma, A. Jannasch, U.-R. Albrecht, K. Hahn, A. Miguel-Lopez, E. Schaeffer, S. Sanchez, Enzyme-powered hollow mesoporous janus nanomotors, *Nano Lett.* 15 (10) (2015) 7043–7050.
- [22] M. Luo, Y. Feng, T. Wang, J. Guan, Micro-/Nanorobots at work in active drug delivery, *Adv. Funct. Mater.* 28 (25) (2018).
- [23] T.Y. Yang, L.J. Wei, L.Y. Jing, J.F. Liang, X.M. Zhang, M. Tang, M.J. Monteiro, Y. Chen, Y. Wang, S. Gu, D.Y. Zhao, H.Q. Yang, J. Liu, G.Q.M. Lu, Dumbbell-shaped Bi-component mesoporous janus solid nanoparticles for biphasic interface catalysis, *Angew. Chem. Int. Ed.* 56 (29) (2017) 8459–8463.
- [24] F. Liu, S. Goyal, M. Forrester, T. Ma, K. Miller, Y. Mansoorieh, J. Henjum, L. Zhou, E. Cochran, S. Jiang, Self-assembly of janus dumbbell nanocrystals and their enhanced surface plasmon resonance, *Nano Lett.* 19 (3) (2019) 1587–1594.
- [25] C.J. Kang, A. Honciuc, Influence of geometries on the assembly of snowman-shaped janus nanoparticles, *ACS Nano* 12 (4) (2018) 3741–3750.
- [26] B. Liu, J.G. Liu, F.X. Liang, Q. Wang, C.L. Zhang, X.Z. Qu, J.L. Li, D. Qiu, Z.Z. Yang, Robust anisotropic composite particles with tunable janus balance, *Macromolecules* 45 (12) (2012) 5176–5184.
- [27] I. Schick, S. Lorenz, D. Gehrig, A.-M. Schilsmann, H. Bauer, M. Panthoefer, K. Fischer, D. Strand, F. Laquai, W. Tremel, Multifunctional two-photon active silica-coated Au@MnO janus particles for selective dual functionalization and imaging, *J. Am. Chem. Soc.* 136 (6) (2014) 2473–2483.
- [28] R. Deng, F. Liang, P. Zhou, C. Zhang, X. Qu, Q. Wang, J. Li, J. Zhu, Z. Yang, Janus nanodisc of diblock copolymers, *Adv. Mater.* 26 (26) (2014), 4469–+.
- [29] Y. Chen, F. Liang, H. Yang, C. Zhang, Q. Wang, X. Qu, J. Li, Y. Cai, D. Qiu, Z. Yang, Janus nanosheets of polymer-inorganic layered composites, *Macromolecules* 45 (3) (2012) 1460–1467.
- [30] K. Chaudhary, Q. Chen, J.J. Juarez, S. Granick, J.A. Lewis, Janus colloidal matchsticks, *J. Am. Chem. Soc.* 134 (31) (2012) 12901–12903.
- [31] J. Yan, K. Chaudhary, S.C. Bae, J.A. Lewis, S. Granick, Colloidal ribbons and rings from Janus magnetic rods, *Nat. Commun.* 4 (2013).
- [32] T. Hessberger, L.B. Braun, R. Zentel, Interfacial self-assembly of amphiphilic dual temperature responsive actuating janus particles, *Adv. Funct. Mater.* 28 (21) (2018) 1800629.
- [33] Y.D. Han, H.-S. Kim, Y.M. Park, H.J. Chun, J.-H. Kim, H.C. Yoon, Retroreflective janus microparticle as a nonspectroscopic optical immunosensing probe, *ACS Appl. Mater. Interfaces* 8 (17) (2016) 10767–10774.
- [34] X. Ma, K. Hahn, S. Sanchez, Catalytic mesoporous janus nanomotors for active cargo delivery, *J. Am. Chem. Soc.* 137 (15) (2015) 4976–4979.
- [35] M. Feyen, C. Weidenthaler, F. Schueth, A.-H. Lu, Regioselectively controlled synthesis of colloidal mushroom nanostructures and their hollow derivatives, *J. Am. Chem. Soc.* 132 (19) (2010) 6791–6799.
- [36] M. Marquis, J. Davy, A.P. Fang, D. Renard, Microfluidics-assisted diffusion self-assembly: toward the control of the shape and size of pectin hydrogel microparticles, *Biomacromolecules* 15 (5) (2014) 1568–1578.
- [37] F. Liang, C. Zhang, Z. Yang, Rational design and synthesis of janus composites, *Adv. Mater.* 26 (40) (2014) 6944–6949.
- [38] J.-B. Fan, Y. Song, H. Liu, Z. Lu, F. Zhang, H. Liu, J. Meng, L. Gu, S. Wang, L. Jiang, A general strategy to synthesize chemically and topologically anisotropic Janus particles, *Sci. Adv.* 3 (6) (2017), e1603203.
- [39] Z. Wu, L. Li, T. Liao, X. Chen, W. Jiang, W. Luo, J. Yang, Z. Sun, Janus nanoarchitectures: from structural design to catalytic applications, *Nano Today* 22 (2018) 62–82.
- [40] K. Kim, J.H. Guo, Z.X. Liang, D.L. Fan, Artificial micro/nanomachines for bioapplications: biochemical delivery and diagnostic sensing, *Adv. Funct. Mater.* 28 (25) (2018) 1705867.
- [41] S. Yang, F. Guo, B. Kiraly, X. Mao, M. Lu, K.W. Leong, T.J. Huang, Microfluidic synthesis of multifunctional Janus particles for biomedical applications, *Lab Chip* 12 (12) (2012) 2097–2102.
- [42] J. Wu, X. Wei, J. Gan, L. Huang, T. Shen, J. Lou, B. Liu, J.X.J. Zhang, K. Qian, Multifunctional magnetic particles for combined circulating tumor cells isolation and cellular metabolism detection, *Adv. Funct. Mater.* 26 (22) (2016) 4016–4025.
- [43] B. Liu, Y. Li, H. Wan, L. Wang, W. Xu, S. Zhu, Y. Liang, B. Zhang, J. Lou, H. Dai, K. Qian, High performance, multiplexed lung cancer biomarker detection on a plasmonic gold chip, *Adv. Funct. Mater.* 26 (44) (2016) 7994–8002.
- [44] J. Liu, T. Liu, J. Pan, S. Liu, G.Q. Lu, Advances in multicompartment mesoporous silica micro/nanoparticles for theranostic applications, *Annu. Rev. Cell Biol.* 9 (1) (2018) 389–411.
- [45] J.R. Gan, X. Wei, Y.X. Li, J. Wu, K. Qian, B.H. Liu, Designer SiO<sub>2</sub>@Au nanoshells towards sensitive and selective detection of small molecules in laser desorption ionization mass spectrometry, *Nanomed-Nanotechnol.* 11 (7) (2015) 1715–1723.
- [46] K. Qian, L. Zhou, J. Zhang, C. Lei, C. Yu, A combo-pore approach for the programmable extraction of peptides/proteins, *Nanoscale* 6 (10) (2014) 5121–5125.
- [47] X.M. Li, L. Zhou, Y. Wei, A.M. El-Toni, F. Zhang, D.Y. Zhao, Anisotropic growth-induced synthesis of dual-compartment janus mesoporous silica nanoparticles for bimodal triggered drugs delivery, *J. Am. Chem. Soc.* 136 (42) (2014) 15086–15092.
- [48] L. Zhang, M. Zhang, L. Zhou, Q. Han, X. Chen, S. Li, L. Li, Z. Su, C. Wang, Dual drug delivery and sequential release by amphiphilic Janus nanoparticles for liver cancer therapeutics, *Biomaterials* 181 (2018) 113–125.
- [49] Z. Wang, D. Shao, Z.M. Chang, M.M. Lu, Y.S. Wang, J. Yue, D. Yang, M.Q. Li, Q.B. Xu, W.F. Dong, Janus gold nanoplatform for synergistic chemoradiotherapy and computed tomography imaging of hepatocellular carcinoma, *ACS Nano* 11 (12) (2017) 12732–12741.
- [50] A. Sanchez, K. Ovejero Paredes, J. Ruiz-Cabello, P. Martinez-Ruiz, J. Manuel Pingarron, R. Villalonga, M. Filice, Hybrid decorated Core@Shell janus nanoparticles as a flexible platform for targeted multimodal molecular bioimaging of cancer, *ACS Appl. Mater. Interfaces* 10 (37) (2018) 31032–31043.
- [51] T. Sheng, Z. Xie, P. Liu, J. Chen, S. Chen, H. Ding, J. Deng, Y. Yuan, D. Deng, Magnetic encoding plasmonic janus microbead-based suspension array for high sensitivity multiplex analysis, *Adv. Mater. Interfaces* 5 (19) (2018) 1800343.
- [52] K. Lee, Y. Yi, Y. Yu, Remote control of T cell activation using magnetic janus particles, *Angew. Chem. Int. Ed.* 55 (26) (2016) 7384–7387.
- [53] B. Jurado-Sanchez, M. Pacheco, J. Rojo, A. Escarpa, Magnetocatalytic graphene quantum dots janus micromotors for bacterial endotoxin detection, *Angew. Chem. Int. Ed.* 56 (24) (2017) 6957–6961.
- [54] C.R. Chen, E. Karshalev, J.X. Li, F. Soto, R. Castillo, I. Campos, F.Z. Mou, J.G. Guan, J. Wang, Transient micromotors that disappear when No longer needed, *ACS Nano* 10 (11) (2016) 10389–10396.
- [55] J. He, M.J. Hourwitz, Y. Liu, M.T. Perez, Z. Nie, One-pot facile synthesis of Janus particles with tailored shape and functionality, *Chem. Commun.* 47 (46) (2011) 12450–12452.
- [56] A. Kuijk, A. van Blaaderen, A. Imhof, Synthesis of monodisperse, rodlike silica colloids with tunable aspect ratio, *J. Am. Chem. Soc.* 133 (8) (2011) 2346–2349.
- [57] R. Zhao, X. Yu, D. Sun, L. Huang, F. Liang, Z. Liu, Functional janus particles modified with ionic liquids for dye degradation, *ACS Appl. Nano Mater.* 2 (4) (2019) 2127–2132.
- [58] Y. Jin, X. Gao, Plasmonic fluorescent quantum dots, *Nat. Nanotechnol.* 4 (9) (2009) 571–576.
- [59] Y. Song, J. Zhou, J.-B. Fan, W. Zhai, J. Meng, S. Wang, Hydrophilic/oleophilic magnetic janus particles for the rapid and efficient oil-water separation, *Adv. Funct. Mater.* 28 (32) (2018) 1802493.
- [60] Y. Song, S. Chen, Janus nanoparticles: preparation, characterization, and applications, *Chem. Asian J.* 9 (2) (2014) 418–430.
- [61] J. Faria, M.P. Ruiz, D.E. Resasco, Phase-selective catalysis in emulsions stabilized by janus silica-nanoparticles, *Adv. Synth. Catal.* 352 (14–15) (2010) 2359–2364.
- [62] S. Fujii, Y. Yokoyama, Y. Miyanari, T. Shiono, M. Ito, S.-i. Yusa, Y. Nakamura, Micrometer-sized gold-silica janus particles as particulate emulsifiers, *Langmuir* 29 (18) (2013) 5457–5465.
- [63] T. Zhao, X. Zhu, C.-T. Hung, P. Wang, A. Elzatahy, A.A. Al-Khalaf, W.N. Hozzein, F. Zhang, X. Li, D. Zhao, Spatial isolation of carbon and silica in a single janus mesoporous nanoparticle with tunable amphiphilicity, *J. Am. Chem. Soc.* 140 (31) (2018) 10009–10015.
- [64] Z.W. Seh, S. Liu, S.-Y. Zhang, M.S. Bharathi, H. Ramanarayanan, M. Low, K.W. Shah, Y.-W. Zhang, M.-Y. Han, Anisotropic growth of titania onto various gold nanostructures: synthesis, theoretical understanding, and optimization for catalysis, *Angew. Chem. Int. Ed.* 50 (43) (2011) 10140–10143.
- [65] M.D. McConnell, M.J. Kraeutler, S. Yang, R.J. Composto, Patchy and multiregion janus particles with tunable optical properties, *Nano Lett.* 10 (2) (2010) 603–609.

- [66] E. Shaviv, O. Schubert, M. Alves-Santos, G. Goldoni, R. Di Felice, F. Vallée, N. Del Fatti, U. Banin, C. Sönichsen, Absorption properties of metal-semiconductor hybrid nanoparticles, *ACS Nano* 5 (6) (2011) 4712–4719.
- [67] Y. Zhang, M. Long, P. Huang, H. Yang, S. Chang, Y. Hu, A. Tang, L. Mao, Emerging integrated nanoclay-facilitated drug delivery system for papillary thyroid cancer therapy, *Sci. Rep.* 6 (2016) 33335.
- [68] S.-H. Hu, X. Gao, Nanocomposites with spatially separated functionalities for combined imaging and magnetolytic therapy, *J. Am. Chem. Soc.* 132 (21) (2010) 7234–7237.
- [69] J. Jiang, H. Gu, H. Shao, E. Devlin, G.C. Papaefthymiou, J.Y. Ying, Bifunctional  $\text{Fe}_3\text{O}_4$ -Ag heterodimer nanoparticles for two-photon fluorescence imaging and magnetic manipulation, *Adv. Mater.* 20 (23) (2008) 4403–4407.
- [70] K.C. Bryson, T.I. Löbling, A.H.E. Müller, T.P. Russell, R.C. Hayward, Using janus nanoparticles to trap polymer blend morphologies during solvent-evaporation-induced demixing, *Macromolecules* 48 (12) (2015) 4220–4227.
- [71] R. Bahrami, T.I. Löbling, A.H. Gröschel, H. Schmalz, A.H.E. Müller, V. Altstädt, The impact of janus nanoparticles on the compatibilization of immiscible polymer blends under technologically relevant conditions, *ACS Nano* 8 (10) (2014) 10048–10056.
- [72] A.S. Caro, T. Parpate, B. Otazaghine, A. Taguet, J.M. Lopez-Cuesta, Viscoelastic properties of polystyrene/polyamide-6 blend compatibilized with silica/polystyrene Janus hybrid nanoparticles, *J. Rheol.* 61 (2) (2017) 305–310.
- [73] S. Khoei, A. Nouri, Chapter 4 - preparation of Janus nanoparticles and its application in drug delivery, in: A.M. Grumezescu (Ed.), *Design and Development of New Nanocarriers*, William Andrew Publishing, 2018, pp. 145–180.
- [74] C. Xu, J. Xie, D. Ho, C. Wang, N. Kohler, E.G. Walsh, J.R. Morgan, Y.E. Chin, S. Sun,  $\text{Au}-\text{Fe}_3\text{O}_4$  dumbbell nanoparticles as dual-functional probes, *Angew. Chem. Int. Ed.* 47 (1) (2008) 173–176.
- [75] Z. Xu, Y. Hou, S. Sun, Magnetic core/shell  $\text{Fe}_3\text{O}_4/\text{Au}$  and  $\text{Fe}_3\text{O}_4/\text{Au}/\text{Ag}$  nanoparticles with tunable plasmonic properties, *J. Am. Chem. Soc.* 129 (28) (2007) 8698–8699.
- [76] C. Tang, C. Zhang, J. Liu, X. Qu, J. Li, Z. Yang, Large scale synthesis of janus submicrometer sized colloids by seeded emulsion polymerization, *Macromolecules* 43 (11) (2010) 5114–5120.
- [77] X. Fan, J. Yang, X.J. Loh, Z. Li, Polymeric janus nanoparticles: recent advances in synthetic strategies, materials properties, and applications, *macromol. Rapid Commun.* 40 (5) (2019) 1800203.
- [78] K.H. Ku, Y.J. Lee, G.-R. Yi, S.G. Jang, B.V.K.J. Schmidt, K. Liao, D. Klinger, C.J. Hawker, B.J. Kim, Shape-tunable biphasic janus particles as pH-responsive switchable surfactants, *Macromolecules* 50 (23) (2017) 9276–9285.
- [79] R. Deng, F. Liang, X. Qu, Q. Wang, J. Zhu, Z. Yang, Diblock copolymer based janus nanoparticles, *Macromolecules* 48 (3) (2015) 750–755.
- [80] S. Bhaskar, K.M. Pollock, M. Yoshida, J. Lahann, Towards designer microparticles: simultaneous control of anisotropy, shape, and size, *Small* 6 (3) (2010) 404–411.
- [81] X. Li, T. Zhao, Y. Lu, P. Wang, A.M. El-Toni, F. Zhang, D. Zhao, Degradation-restructuring induced anisotropic epitaxial growth for fabrication of asymmetric diblock and triblock mesoporous nanocomposites, *Adv. Mater.* 29 (30) (2017) 1701652.
- [82] L.R. Rowe, B.S. Chapman, J.B. Tracy, Understanding and controlling the morphology of silica shells on gold nanorods, *Chem. Mater.* 30 (18) (2018) 6249–6258.
- [83] H. Jia, A. Du, H. Zhang, J. Yang, R. Jiang, J. Wang, C.-y. Zhang, Site-selective growth of crystalline ceria with oxygen vacancies on gold nanocrystals for near-infrared nitrogen photofixation, *J. Am. Chem. Soc.* 141 (13) (2019) 5083–5086.
- [84] D. Nagao, K. Goto, H. Ishii, M. Konno, Preparation of asymmetrically nanoparticle-supported, monodisperse composite dumbbells by protruding a smooth polymer bulge from rugged spheres, *Langmuir* 27 (21) (2011) 13302–13307.
- [85] L. Qu, H. Hu, J. Yu, X. Yu, J. Liu, Y. Xu, Q. Zhang, High-yield synthesis of janus dendritic mesoporous silica@resorcinol-formaldehyde nanoparticles: a competing growth mechanism, *Langmuir* 33 (21) (2017) 5269–5274.
- [86] S. Ye, R.L. Carroll, Design and fabrication of bimetallic colloidal "janus" particles, *ACS Appl. Mater. Interfaces* 2 (3) (2010) 616–620.
- [87] C.-C. Lin, C.-W. Liao, Y.-C. Chao, C. Kuo, Fabrication and characterization of asymmetric janus and ternary particles, *ACS Appl. Mater. Interfaces* 2 (11) (2010) 3185–3191.
- [88] A. Ayala, C. Carbonell, I. Imaz, D. Maspoch, Introducing asymmetric functionality into MOFs via the generation of metallic Janus MOF particles, *Chem. Commun.* 52 (29) (2016) 5096–5099.
- [89] J. Gong, X. Zu, Y. Li, W. Mu, Y. Deng, Janus particles with tunable coverage of zinc oxide nanowires, *J. Mater. Chem.* 21 (7) (2011) 2067–2069.
- [90] Q. Zhang, L. Zhang, S. Li, X. Chen, M. Zhang, T. Wang, L. Li, C. Wang, Designed synthesis of  $\text{Au}/\text{Fe}_3\text{O}_4/\text{C}$  janus nanoparticles for dual-modal imaging and actively targeted chemo-photothermal synergistic therapy of cancer cells, *Chem. Eur. J.* 23 (68) (2017) 17242–17248.
- [91] R.H. Staff, J. Willersinn, A. Musyanovych, K. Landfester, D. Crespy, Janus nanoparticles with both faces selectively functionalized for click chemistry, *Polym. Chem.* 5 (13) (2014) 4097–4104.
- [92] H. Zhang, J.K. Nunes, S.E.A. Gratton, K.P. Herlihy, P.D. Pohlhaus, J.M. DeSimone, Fabrication of multiphasic and regio-specifically functionalized PRINT®-particles of controlled size and shape, *New J. Phys.* 11 (7) (2009), 075018.
- [93] F. Chang, B.G.P. van Ravenstein, K.S. Lacina, W.K. Kegel, Bifunctional janus spheres with chemically orthogonal patches, *ACS Macro Lett.* 8 (6) (2019) 714–718.
- [94] A. Kirillova, C. Marschelke, A. Syntska, Hybrid janus particles: challenges and opportunities for the design of active functional interfaces and surfaces, *ACS Appl. Mater. Interfaces* 11 (10) (2019) 9643–9671.
- [95] L. Wang, M. Pan, S. Song, L. Zhu, J. Yuan, G. Liu, Intriguing morphology evolution from noncrosslinked poly(tertbutyl acrylate) seeds with polar functional groups in soap-free emulsion polymerization of styrene, *Langmuir* 32 (31) (2016) 7829–7840.
- [96] M. Urban, B. Freisinger, O. Ghazy, R. Staff, K. Landfester, D. Crespy, A. Musyanovych, Polymer janus nanoparticles with two spatially segregated functionalizations, *Macromolecules* 47 (20) (2014) 7194–7199.
- [97] Y. Yin, S. Zhou, B. You, L. Wu, Facile fabrication and self-assembly of polystyrene-silica asymmetric colloid spheres, *J. Polym. Sci., Polym. Chem. Ed.* 49 (15) (2011) 3272–3279.
- [98] C. Wang, H. Yin, S. Dai, S. Sun, A general approach to noble metal-metal oxide dumbbell nanoparticles and their catalytic application for CO oxidation, *Chem. Mater.* 22 (10) (2010) 3277–3282.
- [99] J.H. Schroeder, M. Doroshenko, D. Pirner, M.E.J. Mauer, B. Foerster, V. Boyko, B. Reck, K.J. Roschmann, A.H.E. Mueller, S. Foerster, Interfacial stabilization by soft Janus nanoparticles, *Polymer* 106 (2016) 208–217.
- [100] R. Deng, S. Liu, F. Liang, K. Wang, J. Zhu, Z. Yang, Polymeric janus particles with hierarchical structures, *Macromolecules* 47 (11) (2014) 3701–3707.
- [101] S. Lone, S.H. Kim, S.W. Nam, S. Park, J. Joo, I.W. Cheong, Microfluidic synthesis of Janus particles by UV-directed phase separation, *Chem. Commun.* 47 (9) (2011) 2634–2636.
- [102] S. Lone, S.H. Kim, S.W. Nam, S. Park, I.W. Cheong, Microfluidic preparation of dual stimuli-responsive microparticles and light-directed clustering, *Langmuir* 26 (23) (2010) 17975–17980.
- [103] T.M. Ruhland, H.S. McKenzie, T.S. Skelton, S.A.F. Bon, A. Walther, A.H.E. Mueller, Nanoscale hybrid silica/polymer Janus particles with a double-responsive hemicorona, *Polymer* 79 (2015) 299–308.
- [104] J. Yuan, W. Zhao, M. Pan, L. Zhu, Self-assembled colloidal particle clusters from in situ pickering-like emulsion polymerization via single electron transfer mechanism, *Macromol. Rapid Commun.* 37 (15) (2016) 1282–1287.
- [105] D. Wei, L. Ge, S. Lu, J. Li, R. Guo, Janus particles templated by janus emulsions and application as a pickering emulsifier, *Langmuir* 33 (23) (2017) 5819–5828.
- [106] S.G. Kwon, G. Krylova, P.J. Phillips, R.F. Klie, S. Chattopadhyay, T. Shibata, E.E. Bunel, Y. Liu, V.B. Prakapenka, B. Lee, E.V. Shevchenko, Heterogeneous nucleation and shape transformation of multicomponent metallic nanostructures, *Nat. Mater.* 14 (2) (2015) 215–223.
- [107] X. Li, L. Zhou, Y. Wei, A.M. El-Toni, F. Zhang, D. Zhao, Anisotropic encapsulation-induced synthesis of asymmetric single-hole mesoporous nanocages, *J. Am. Chem. Soc.* 137 (18) (2015) 5903–5906.
- [108] X. Wang, Y. He, C. Liu, Y. Liu, Z.-A. Qiao, Q. Huo, A controllable asymmetrical/symmetrical coating strategy for architectural mesoporous organosilica nanostructures, *Nanoscale* 8 (28) (2016) 13581–13588.
- [109] H. Hu, J. Liu, J. Yu, X. Wang, H. Zheng, Y. Xu, M. Chen, J. Han, Z. Liu, Q. Zhang, Synthesis of Janus Au@periodic mesoporous organosilica (PMO) nanostructures with precisely controllable morphology: a seed-shape defined growth mechanism, *Nanoscale* 9 (14) (2017) 4826–4834.
- [110] E. Galati, M. Tebbe, A. Querejeta-Fernandez, H.L. Xin, O. Gang, E.B. Zhulina, E. Kumacheva, Shape-specific patterning of polymer-functionalized nanoparticles, *ACS Nano* 11 (5) (2017) 4995–5002.
- [111] Y. Wang, T. Ding, J.J. Baumberg, S.K. Smoukov, Symmetry breaking polymerization: one-pot synthesis of plasmonic hybrid Janus nanoparticles, *Nanoscale* 7 (23) (2015) 10344–10349.
- [112] S. Torza, S.G. Mason, Three-phase interactions in shear and electrical fields, *J. Colloid Interface Sci.* 33 (1) (1970) 67–83.
- [113] S. Xing, Y. Feng, Y.Y. Tay, T. Chen, J. Xu, M. Pan, J. He, H.H. Hng, Q. Yan, H. Chen, Reducing the symmetry of bimetallic Au@Ag nanoparticles by exploiting eccentric polymer shells, *J. Am. Chem. Soc.* 132 (28) (2010) 9537–9539.
- [114] L. Li, L. Zhang, S. Xing, T. Wang, S. Luo, X. Zhang, C. Liu, Z. Su, C. Wang, Generalized approach to the synthesis of reversible concentric and eccentric polymer-coated nanostructures, *Small* 9 (6) (2013) 825–830.
- [115] F. Tang, L. Li, D. Chen, Mesoporous silica nanoparticles: synthesis, biocompatibility and drug delivery, *Adv. Mater.* 24 (12) (2012) 1504–1534.
- [116] J. Wen, K. Yang, F. Liu, H. Li, Y. Xu, S. Sun, Diverse gatekeepers for mesoporous silica nanoparticle based drug delivery systems, *Chem. Soc. Rev.* 46 (19) (2017) 6024–6045.
- [117] J. Liu, N.P. Wickramaratne, S.Z. Qiao, M. Jaroniec, Molecular-based design and emerging applications of nanoporous carbon spheres, *Nat. Mater.* 14 (8) (2015) 763–774.
- [118] H. Wang, Q.W. Chen, S.Q. Zhou, Carbon-based hybrid nanogels: a synergistic nanoplatform for combined biosensing, bioimaging, and responsive drug delivery, *Chem. Soc. Rev.* 47 (11) (2018) 4198–4232.
- [119] C. Rejeeth, R. Vivek, V. NipunBabu, A. Sharma, X. Ding, K. Qian, Cancer nanomedicine: from PDGF targeted drug delivery, *MedChemComm* 8 (11) (2017) 2055–2059.
- [120] L.-S. Lin, X. Yang, Z. Zhou, Z. Yang, O. Jacobson, Y. Liu, A. Yang, G. Niu, J. Song, H.-H. Yang, X. Chen, Yolk-shell nanostructure: an ideal architecture to achieve harmonious integration of magnetic-plasmonic hybrid theranostic platform, *Adv. Mater.* 29 (21) (2017) 1606681.
- [121] J. Song, X. Yang, Z. Yang, L. Lin, Y. Liu, Z. Zhou, Z. Shen, G. Yu, Y. Dai, O. Jacobson, J. Munasinghe, B. Yung, G.-J. Teng, X. Chen, Rational design of branched nanoporous gold nanoshells with enhanced physico-optical properties for optical imaging and cancer therapy, *ACS Nano* 11 (6) (2017) 6102–6113.
- [122] R.G. Chaudhuri, S. Paria, Core/shell nanoparticles: classes, properties, synthesis mechanisms, characterization, and applications, *Chem. Rev.* 112 (4) (2012) 2373–2433.

- [123] J. Liu, S.Z. Qiao, J.S. Chen, X.W. Lou, X.R. Xing, G.Q. Lu, Yolk/shell nanoparticles: new platforms for nanoreactors, drug delivery and lithium-ion batteries, *Chem. Commun.* 47 (47) (2011) 12578–12591.
- [124] X.J. Cai, W. Gao, M. Ma, M.Y. Wu, L.L. Zhang, Y.Y. Zheng, H.R. Chen, J.L. Shi, A prussian blue-based core-shell hollow-structured mesoporous nanoparticle as a smart theranostic agent with ultrahigh pH-responsive longitudinal relaxivity, *Adv. Mater.* 27 (41) (2015), 6382–.
- [125] Y. Li, J. Shi, Hollow-structured mesoporous materials: chemical synthesis, functionalization and applications, *Adv. Mater.* 26 (20) (2014) 3176–3205.
- [126] E. Dehghani, M. Salami-Kalajahi, H. Roghani-Mamaqani, Fabricating cauliflower-like and dumbbell-like Janus particles: loading and simultaneous release of DOX and ibuprofen, *Colloids Surfaces B Biointerfaces* 173 (2019) 155–163.
- [127] E. Dehghani, M. Salami-Kalajahi, H. Roghani-Mamaqani, Simultaneous two drugs release form Janus particles prepared via polymerization-induced phase separation approach, *Colloids Surfaces B Biointerfaces* 170 (2018) 85–91.
- [128] M. Fallahi-Sambaran, M. Salami-Kalajahi, E. Dehghani, F. Abbasi, Investigation of different core-shell toward Janus morphologies by variation of surfactant and feeding composition: a study on the kinetics of DOX release, *Colloids Surfaces B Biointerfaces* 170 (2018) 578–587.
- [129] Y. Xing, M. Zhou, X. Du, X. Li, J. Li, T. Xu, X. Zhang, Hollow mesoporous carbon@Pt Janus nanomotors with dual response of  $H_2O_2$  and near-infrared light for active cargo delivery, *Appl. Mater. Today* 17 (2019) 85–91.
- [130] S. Li, L. Zhang, X. Liang, T. Wang, X. Chen, C. Liu, L. Li, C. Wang, Tailored synthesis of hollow MOF/polydopamine Janus nanoparticles for synergistic multi-drug chemo-photothermal therapy, *Chem. Eng. J.* 378 (2019) 122175.
- [131] Z. Wang, Z.M. Chang, M.M. Lu, D. Shao, J. Yue, D. Yang, M.Q. Li, W.F. Dong, Janus silver/silica nanoplateforms for light-activated liver cancer chemo/photothermal therapy, *ACS Appl. Mater. Interfaces* 9 (36) (2017) 30306–30317.
- [132] Z. Wang, F. Zhang, D. Shao, Z. Chang, L. Wang, H. Hu, X. Zheng, X. Li, F. Chen, Z. Tu, M. Li, W. Sun, L. Chen, W.-F. Dong, Janus nanobullets combine photodynamic therapy and magnetic hyperthermia to potentiate synergistic anti-metastatic immunotherapy, *Adv. Sci. O (0)* (2019) 1901690.
- [133] S. Liang, X. Deng, Y. Chang, C. Sun, S. Shao, Z. Xie, X. Xiao, P.a. Ma, H. Zhang, Z. Cheng, J. Lin, Intelligent hollow Pt-CuS janus architecture for synergistic catalysis-enhanced sonodynamic and photothermal cancer therapy, *Nano Lett.* 19 (6) (2019) 4134–4145.
- [134] Z. Chen, T. Xia, Z. Zhang, S. Xie, T. Wang, X. Li, Enzyme-powered Janus nanomotors launched from intratumoral depots to address drug delivery barriers, *Chem. Eng. J.* 375 (2019) 122109.
- [135] V. Sridhar, B.-W. Park, M. Sitti, Light-driven janus hollow mesoporous  $TiO_2$ -Au microswimmers, *Adv. Funct. Mater.* 28 (25) (2018) 1704902.
- [136] F.Z. Mou, C.R. Chen, Q. Zhong, Y.X. Yin, H.R. Ma, J.G. Guan, Autonomous motion and temperature-controlled drug delivery of Mg/Pt-poly(N-isopropylacrylamide) janus micromotors driven by simulated body fluid and blood plasma, *ACS Appl. Mater. Interfaces* 6 (12) (2014) 9897–9903.
- [137] Y. Wu, X. Lin, Z. Wu, H. Moehwald, Q. He, Self-propelled polymer multilayer janus capsules for effective drug delivery and light-triggered release, *ACS Appl. Mater. Interfaces* 6 (13) (2014) 10476–10481.
- [138] S.J. Patel, N.E. Sanjana, R.J. Kishton, A. Egidizadeh, S.K. Vodnala, M. Cam, J.J. Gartner, L. Jia, S.M. Steinberg, T.N. Yamamoto, A.S. Merchant, G.U. Mehta, A. Chichura, O. Shalem, E. Tran, R. Eil, M. Sukumar, E.P. Guijarro, C.-P. Day, P. Robbins, S. Feldman, G. Merlini, F. Zhang, N.P. Restifo, Identification of essential genes for cancer immunotherapy, *Nature* 548 (7669) (2017), 537–.
- [139] S.L. Buchan, A. Rogel, A. Al-Shamkhani, The immunobiology of CD27 and OX40 and their potential as targets for cancer immunotherapy, *Blood* 131 (1) (2018) 39–48.
- [140] S. Gai, G. Yang, P. Yang, F. He, J. Lin, D. Jin, B. Xing, Recent advances in functional nanomaterials for light-triggered cancer therapy, *Nano Today* 19 (2018) 146–187.
- [141] D.-E. Lee, H. Koo, I.-C. Sun, J.H. Ryu, K. Kim, I.C. Kwon, Multifunctional nanoparticles for multimodal imaging and theragnosis, *Chem. Soc. Rev.* 41 (7) (2012) 2656–2672.
- [142] Y. Ju, H. Zhang, J. Yu, S. Tong, N. Tian, Z. Wang, X. Wang, X. Su, X. Chu, J. Lin, Y. Ding, G. Li, F. Sheng, Y. Hou, Monodisperse Au-Fe2C janus nanoparticles: an attractive multifunctional material for triple-modal imaging-guided tumor photothermal therapy, *ACS Nano* 11 (9) (2017) 9239–9248.
- [143] N. Lee, S.H. Choi, T. Hyeon, Nano-sized CT contrast agents, *Adv. Mater.* 25 (19) (2013) 2641–2660.
- [144] J.H. Park, D.S. Dumani, A. Arsiwala, S. Emelianov, R.S. Kane, Tunable aggregation of gold-silica janus nanoparticles to enable contrast-enhanced multiwavelength photoacoustic imaging in vivo, *Nanoscale* 10 (32) (2018) 15365–15370.
- [145] G. Song, M. Chen, Y. Zhang, L. Cui, H. Qu, X. Zheng, M. Wintermark, Z. Liu, J. Rao, Janus iron oxides @ semiconducting polymer nanoparticle tracer for cell tracking by magnetic particle imaging, *Nano Lett.* 18 (1) (2018) 182–189.
- [146] M.Z. Iqbal, W. Ren, M. Saeed, T. Chen, X. Ma, X. Yu, J. Zhang, L. Zhang, A. Li, A. Wu, A facile fabrication route for binary transition metal oxide-based Janus nanoparticles for cancer theranostic applications, *Nano Research* 11 (10) (2018) 5735–5750.
- [147] L. Zeng, W. Ren, L. Xiang, J. Zheng, B. Chen, A. Wu, Multifunctional  $Fe_3O_4$ - $TiO_2$  nano composites for magnetic resonance imaging and potential photodynamic therapy, *Nanoscale* 5 (5) (2013) 2107–2113.
- [148] M. Zheng, C. Yue, Y. Ma, P. Gong, P. Zhao, C. Zheng, Z. Sheng, P. Zhang, Z. Wang, L. Cai, Single-step assembly of DOX/ICG loaded lipid-polymer nanoparticles for highly effective chemo-photothermal combination therapy, *ACS Nano* 7 (3) (2013) 2056–2067.
- [149] H. Gong, L. Cheng, J. Xiang, H. Xu, L. Feng, X. Shi, Z. Liu, Near-infrared absorbing polymeric nanoparticles as a versatile drug carrier for cancer combination therapy, *Adv. Funct. Mater.* 23 (48) (2013) 6059–6067.
- [150] Q. Chen, L. Xu, C. Liang, C. Wang, R. Peng, Z. Liu, Photothermal therapy with immune-adjuvant nanoparticles together with checkpoint blockade for effective cancer immunotherapy, *Nat. Commun.* 7 (2016) 13193.
- [151] R. Zhang, C. Rejeeth, W. Xu, C. Zhu, X. Liu, J. Wan, M. Jiang, K. Qian, Label-free electrochemical sensor for CD44 by ligand-protein interaction, *Anal. Chem.* 91 (11) (2019) 7078–7085.
- [152] R. Zhang, B. Le, W. Xu, K. Guo, X. Sun, H. Su, L. Huang, J. Huang, T. Shen, T. Liao, Y. Liang, J.X.J. Zhang, H. Dai, K. Qian, Magnetic “squashing” of circulating tumor cells on plasmonic substrates for ultrasensitive NIR fluorescence detection, *Small Methods* 3 (2) (2019) 1800474.
- [153] L. Huang, J. Wan, X. Wei, Y. Liu, J. Huang, X. Sun, R. Zhang, D.D. Gurav, V. Vedarethinam, Y. Li, R. Chen, K. Qian, Plasmonic silver nanoshells for drug and metabolite detection, *Nat. Commun.* 8 (2017).
- [154] X. Wei, Z.H. Liu, X.L. Jin, L. Huang, D.D. Gurav, X. Sun, B.H. Liu, J. Ye, K. Qian, Plasmonic nanoshells enhanced laser desorption/ionization mass spectrometry for detection of serum metabolites, *Anal. Chim. Acta* 950 (2017) 147–155.
- [155] X.M. Sun, J.J. Wan, K. Qian, Designed microdevices for in vitro diagnostics, *Small Methods* 1 (10) (2017) 1700196.
- [156] G. Maduraiveeran, M. Sasidharan, V. Ganeshan, Electrochemical sensor and biosensor platforms based on advanced nanomaterials for biological and biomedical applications, *Biosens. Bioelectron.* 103 (2018) 113–129.
- [157] L.S. Lin, J.B. Song, H.H. Yang, X.Y. Chen, Yolk-shell nanostructures: design, synthesis, and biomedical applications, *Adv. Mater.* 30 (6) (2018) 1704639.
- [158] S. Sun, R. Wang, Y. Huang, J. Xu, K. Yao, W. Liu, Y. Cao, K. Qian, Design of hierarchical beads for efficient label-free cell capture, *Small* 15 (34) (2019) 1902441.
- [159] D.D. Gurav, Y. Jia, J. Ye, K. Qian, Design of plasmonic nanomaterials for diagnostic spectrometry, *Nanoscale Adv* 1 (2) (2019) 459–469.
- [160] V. Vedarethinam, L. Huang, W. Xu, R. Zhang, D.D. Gurav, X. Sun, J. Yang, R. Chen, K. Qian, Detection and inhibition of bacteria on a dual-functional silver platform, *Small* 15 (3) (2019) 1803051.
- [161] X. Sun, L. Huang, R. Zhang, W. Xu, J. Huang, D.D. Gurav, V. Vedarethinam, R. Chen, J. Lou, Q. Wang, J. Wan, K. Qian, Metabolic fingerprinting on a plasmonic gold chip for mass spectrometry based in vitro diagnostics, *ACS Cent. Sci.* 4 (2) (2018) 223–229.
- [162] S. Wu, L.X. Qian, L. Huang, X.M. Sun, H.Y. Su, D.D. Gurav, M.W. Jiang, W. Cai, K. Qian, A plasmonic mass spectrometry approach for detection of small nutrients and toxins, *Nano-Micro Lett.* 10 (3) (2018) 52.
- [163] C. Rejeeth, X. Pang, R. Zhang, W. Xu, X. Sun, B. Liu, J. Lou, J. Wan, H. Gu, W. Yan, K. Qian, Extraction, detection, and profiling of serum biomarkers using designed  $Fe_3O_4@SiO_2@HA$  core-shell particles, *Nano Res* 11 (1) (2018) 68–79.
- [164] C. Lu, X. Liu, Y. Li, F. Yu, L. Tang, Y. Hu, Y. Yine, Multifunctional janus hematite silica nanoparticles: mimicking peroxidase-like activity and sensitive colorimetric detection of glucose, *ACS Appl. Mater. Interfaces* 7 (28) (2015) 15395–15402.
- [165] H. Su, T. Liu, L. Huang, J. Huang, J. Cao, H. Yang, J. Ye, J. Liu, K. Qian, Plasmonic Janus hybrids for the detection of small metabolites, *J. Mater. Chem. B* 6 (44) (2018) 7280–7287.
- [166] B. Chen, Y. Jia, Y. Gao, L. Sanchez, S.M. Anthony, Y. Yu, Janus particles as artificial antigen-presenting cells for T cell activation, *ACS Appl. Mater. Interfaces* 6 (21) (2014) 18435–18439.
- [167] K. Perica, A. Tu, A. Richter, J.G. Bieler, M. Edidin, J.P. Schneck, Magnetic field-induced T cell receptor clustering by nanoparticles enhances T cell activation and stimulates antitumor activity, *ACS Nano* 8 (3) (2014) 2252–2260.
- [168] E. Zhang, M.F. Kircher, M. Koch, L. Eliasson, S.N. Goldberg, E. Renstrom, Dynamic magnetic fields remote-control apoptosis via nanoparticle rotation, *ACS Nano* 8 (4) (2014) 3192–3201.
- [169] M.M. Stanton, J. Simmchen, X. Ma, A. Miguel-Lopez, S. Sanchez, Biohybrid janus motors driven by *Escherichia coli*, *Adv. Mater. Interfaces* 3 (2) (2016) 1500505.
- [170] M. Guix, C.C. Mayorga-Martinez, A. Merkoci, Nano/Micromotors in (Bio)Chem. Sci. Applications, *Chem. Rev.* 114 (12) (2014) 6285–6322.
- [171] J. Wang, W. Gao, Nano/microscale motors: biomedical opportunities and challenges, *ACS Nano* 6 (7) (2012) 5745–5751.
- [172] P. Schattling, B. Thingholm, B. Stadler, Enhanced diffusion of glucose-fueled janus particles, *Chem. Mater.* 27 (21) (2015) 7412–7418.
- [173] X. Ma, X. Wang, K. Hahn, S. Sanchez, Motion control of urea-powered biocompatible hollow microcapsules, *ACS Nano* 10 (3) (2016) 3597–3605.